The effects of citral and wortmannin on the morphology and differentiation of the developing mouse tooth

By Roland M. Klar

(0100706V)

A dissertation submitted to the Faculty of Science, University of Witwatersrand, in fulfillment of the requirements for a Masters Degree in the
School of Anatomical Sciences

Declaration

I herby declare that the research done is my personal work. It is being submitted for the Degree of Master of Science, at the University of the Witwatersrand, Johannesburg, to the Faculty of Science; for the School of Anatomical Sciences. It has not been submitted before for any other degree or examination to another University.

Roland Klar

ROLAND M. KLAR

(16 March 2009)

Dedication

I dedicate this work to the College of Science of Wits for having accepted me for a degree in science so that I could make my dreams a reality. To Professor E. Dabbs who was the man that inspired me to do scientific research. Furthermore I would like to dedicate it to Professor B. Fabian and Professor B. Kramer for having shown me the true path of a scientist. I would also like to dedicate this work to my Austrian grandfather and my family.

Acknowledgments

I would like to thank Professor B. Fabian for having assisted me with his ideas in both my research work and the write-up.

To my family --Wolfgang, Lucia, Gerald, Angela, Jessica and Tristan Klar-- though crazed, for their moral support and giving me new hope for each day to fight on in my project.

To my friend Kobus Leach (at Stellenbosch University), for his ongoing sarcasm and mental stimulation. Thank you again for helping me where you could, Kobus, I really appreciate it.

I would also like to thank my colleagues in 2A11 for their support and the “wonderful learning experiences” they have given me throughout this project.

I would also especially like to thank Mrs Leslie York for her advice and assistance in the work and Mrs Hasina Ali for having assisted me in my PCR and to thank Professor C. Allan who helped in checking the statistical calculations.

A special acknowledgement goes to Dr R. Duarte, Dr K. Lightfoot and Dr C. Penny for their assistance in QRT-PCR and letting me use their ABI 7500 machine to do my runs.

I would also like to thank Professor B. Kramer, Professor B. Fabian and Dr Kuykendall for organizing the grant money from the National Research Foundation, which allowed me to undertake this Master of Science.

Contents **Page Number**

Abbreviations

BMP	bone morphogenic protein
cDNA	complementary deoxyribonucleic acid
C_t	threshold cycle
LM	light microscope
DIC	differential interference contrast
DNA	deoxyribonucleic acid
dNTP	deoxynucleotide triphosphate
E	embryo
EGF	epidermal growth factor
FCS	fetal calf serum
FGF	fibroblast growth factor
ICC	immunocytochemistry
KLK	kallikrein
m	messenger
PAP	peroxide anti peroxidase
PBS	phosphate buffered saline
PCR	polymerase chain reaction
PI3K	phosphatidylinositol 3-kinase
QRT	quantitative real-time
RA	retinoic acid
RALDH	retinal dehydrogenase
RNA	ribonucleic acid
UI	international units

List of Tables

List of Figures

Abstract

Odontogenesis has been extensively studied to ascertain the cellular pathways and biochemical signals that help to regulate this developmental system. Various gene families and growth factors that been identified as important regulators of tooth development. However other molecules such as retinoic acid and PI3K have also been implicated in the regulation of tooth development, especially in the initiation stage of tooth development and cusp morphogenesis. By inhibiting RA synthesis with citral, and PI3K activation using wortmannin, the study sought to investigate how amelogenesis and cusp morphogenesis were affected in murine developing first mandibular molars. Tooth development of the 14.5 and 16.5 day embryonic mouse, *in* vitro for 12 days, did not progress beyond the early bell stage. This was indicated by the absence of an enamel layer and possible remnant basement membrane in the cultured molars. Furthermore, no deviations in cusp morphology were observed, when inhibitors against either RA or PI3K were applied. However utilizing QRT-PCR, it was noted that the synthesis of amelogenin-mRNA increased in the 14.5 day tooth explants treated with citral, but not in the 16.5 day molar explants subjected to the same treatment. These results could therefore suggest that the degradative pathways or feedback systems controlling amelogenin-mRNA levels are inactive prior to the onset of amelogenesis on day 15-16. On the other hand, PI3K did not appear to regulate amelogenin expression, in either 14.5 or 16.5 day embryonic mouse molar explants that were treated with wortmannin. Statistical analysis revealed no changes in the laminin α5-mRNA levels in either 14.5 or 16.5 day molars treated with either citral or wortmannin, which suggests that PI3K is not the only cellular pathway that controls laminin-mRNA synthesis.

1. Introduction

1.1 Tooth development

The mechanism of tooth formation is a highly conserved event in the vertebrate kingdom. Derived from stomodeal ectodermal cells of the first pharyngeal arch and ectomesenchyme of the cranial neural crest (Cobourne, 1999; Cobourne and Sharpe, 2003), the teeth develop prenatally, advancing through a chain of morphological stages i.e. bud stage, cap stage and bell stage (Apajalahti, 2004). During these stages, several distinct molecular pathways and processes become active, which are required for normal tooth formation. During infancy, the teeth will erupt from their "incubation chambers" of the maxillary and mandibular arches. During this process, the apical regions are anchored into the alveolar bone of the maxilla and mandible in order to be nourished and maintained (Apajalahti, 2004).

1.1.1 Important morphological events of mouse tooth development:

A.) Initiation stage (Day 10-11)

The initiation stage or dental lamina stage (Fig. 1A) is characterized by the appearance of a continuous band of oral epithelium which forms a horseshoe-shaped thickening along the surfaces of the maxillary and mandibular arches (Moss-Salentijn and Hendricks-Klyvert, 1990). The dental lamina, which gives rise to the teeth, is derived initially from the primary epithelial band (Teaford *et al.*, 2000).

B.) Bud stage (Day 12-13)

The bud stage (Fig. 1B) is characterized by the appearance of an ectodermal bud, which develops from the dental lamina and has no clear cellular arrangement. The dental lamina invades the ectomesenchyme by forming a structure that is rod-like in appearance. These "rods" develop in the position of the future teeth becoming bulbous at their deep ends. They are surrounded by condensed ectomesenchyme. The ectomesenchyme will eventually form the dental follicle and dental papilla (Cohn 1957).

C.) Cap stage (Day 13-14)

The first sign of an arrangement of cells in the developing tooth occurs in the cap stage (Fig. 1C) when the bud separates into two layers, the outer and inner enamel epithelium (Cohn 1957). A blunt angle is created near the junction of the outer and inner enamel epithelial layers, which is referred to as the cervical loop from which the root will form. The residual cellular components of the cap, which occupy the space between the outer and inner enamel epithelia, develop into the stellate reticulum. Thus the enamel organ, which is ultimately responsible for the production of enamel, is composed of inner and outer enamel epithelia and the stellate reticulum. Forming part of the inner enamel epithelium is the primary enamel knot, consisting of non-dividing cells that act as a cell reservoir for the fast-growing enamel organ. This structural knot also serves as an important signalling centre for expressing various growth factors and messenger molecules, of which FGF-4 is the most important (Miletich and Sharpe, 2003). These factors and molecules are necessary for initiating central processes such as amelogenesis.

As tooth development progresses, the primary enamel knot undergoes apoptosis and is replaced by secondary enamel knots. Simultaneously the dental papilla and dental follicle positioned around the bud undergo further condensation with the dental papilla indenting the shallow surface of the bud, forming a “cap” that promotes the elongation of the cervical loop.

D.) Bell stage (Day 15-16)

During the bell stage (Fig. 1D) or differentiation stage, both morphogenesis and cytodifferentiation take place (Moss-Salentijn and Hendricks-Klyvert, 1990), which gives rise to the shape and structure of the tooth. The inner enamel epithelial cells reverse their polarity due to induction by the ectomesenchyme of the dental papilla. The nuclei of these cells relocate towards the apical pole of the cell which is situated away from the basement membrane. Upon polarization, inner enamel epithelial cells stimulate the underlying ectomesenchymal cells of the dental papilla to differentiate into odontoblasts. The odontoblasts then start to secrete dentin and in turn stimulate the inner enamel epithelial cells to differentiate into ameloblasts. Cells lying between the inner enamel epithelium and the stellate reticulum form a layer known as the stratum intermedium, which is believed to assist ameloblasts with enamel formation (Koyama *et al*., 2001). During the bell stage, secondary enamel knots appear which are similar in function to the primary enamel knot, except that they occur in multi-cusped teeth i.e. molars, to assist with the formation of the cusps.

Stage and embryonic day	Main process involved
A.) Initiation stage – Embryonic day 10-11 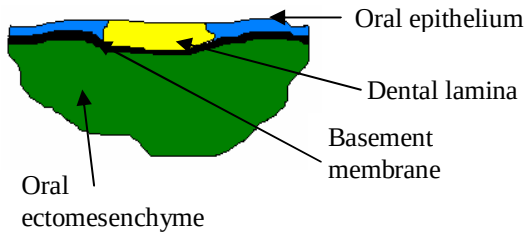	**Induction**
B.) Bud stage – Embryonic day 12-13 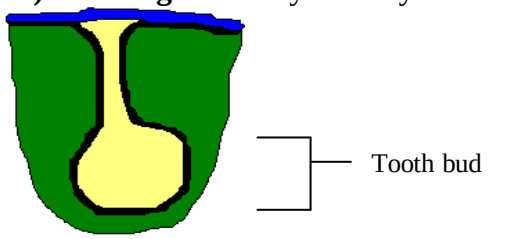	**Proliferation**
C.) Cap stage – Embryonic day 13-14 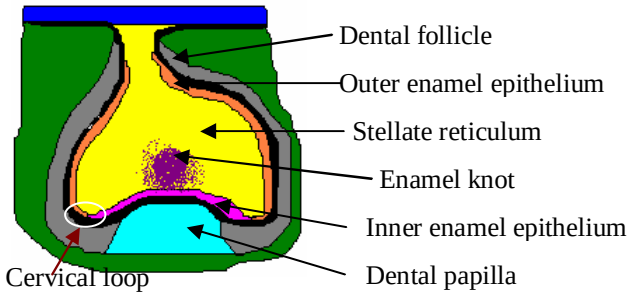	**Proliferation, differentiation, morphogenesis**
D.) Bell stage – Embryonic day 15-16 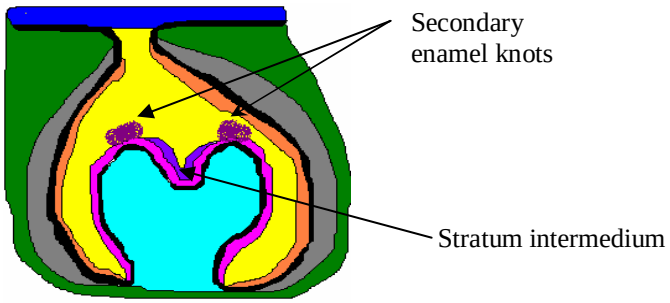	**Proliferation, histodifferentiation, morphodifferentiation**

Figure 1. Diagrammatic representations of the important stages of tooth development (an adjustment from images used by Gilbert (1994))

1.1.2 Amelogenesis

Amelogenesis or enamel formation occurs during the bell stage of tooth development on embryonic days (E) 15-16 in the mouse (Zeichner-David *et al.*, 1995). First the cuboidal cells of the inner enamel epithelium stop dividing. The cells of the inner enamel epithelium then start to elongate and become more columnar in shape and their nuclei migrate to the part of the cell located away from the basement membrane. Classified as pre-ameloblasts, they stimulate the peripheral cells of the dental papilla to differentiate into odontoblasts via an unknown extracellular signal (Moss-Salentijn and Hendricks-Klyvert, 1990). The odontoblasts aggregate into a single layer near the basement membrane and, similarly to the pre-ameloblasts, become polarized (i.e. their nuclei move away from basement membrane). They are incapable of undergoing mitosis and all the organelles for protein synthesis migrate towards the space of the cell facing the basement membrane (Moss-Salentijn and Hendricks-Klyvert, 1990). Once odontoblasts have differentiated and have started synthesizing dentin matrix (Moss-Salentijn and Hendricks-Klyvert, 1990) an unknown messenger molecule is relayed back to the pre-ameloblasts, through the basement membrane, causing the pre-ameloblasts to differentiate into ameloblasts. As this transition occurs the basement membrane is slowly degraded to allow for a connection between the dentin and enamel matrices (Moss-Salentijn and Hendricks-Klyvert, 1990). The ameloblasts then initiate the process of enamel formation, which can be categorized into three stages:

1) Secretory stage of amelogenesis

In the secretory stage of amelogenesis in mouse, specific enamel matrix proteins are released from the rough endoplasmic reticulum of the ameloblasts. These are then secreted by the Tomes process, situated at the apical tip of the polarized ameloblasts, into the extracellular matrix located opposite to the developing dentin matrix. This enamel matrix comprises several scaffolding proteins, of which 90% are amelogenin (Stephanopoulos *et al*., 2005) and the residual consists of ameloblastin, enamelin and tuftelin, which are essential proteins upon which the final mineralization process takes place. Before these proteins are released into the enamel matrix they are post-translationally modified by proteolytic enzymes through cleavage of either the N- or C-terminal of their amino acid peptides (Stephanopoulos *et al*., 2005). The enamel matrix proteins maintain their structural arrangement until the mineralization or maturation stage commences, which starts after a short intermediate step, i.e. the transition stage.

2) Transition stage

As this stage implies, it is a short period at the end of the secretory stage when 50% of the ameloblast cell numbers are reduced by apoptosis (Moss-Salentijn and Hendricks-Klyvert, 1990; Avery, 2001). Furthermore, ameloblasts lose their organelles for protein synthesis, such as the Golgi apparatus, and undergo morphological changes which transform them from a secretory cell into one similar to an epithelial cell involved in ion transport (Avery, 2001).

3) Maturation stage of amelogenesis

The maturation stage is characterized by the enamel matrix becoming fully mineralized (Avery, 2001). The majority of the amelogenin, ameloblastin, enamelin and water (organic) is degraded and is replaced with hydroxyappatite crystals including calcium-and phosphate ions (inorganic) which accumulate in the spaces left by the organic matrix. The maturation is an ongoing process that begins as soon as some enamel matrix has been formed (Moss-Salentijn and Hendricks-Klyvert, 1990). Yet, the complete maturation of enamel is only achieved once all mineralization has occurred and almost all the organic molecules in the enamel have been removed (Avery, 2001).

1.2 Identification of genes involved in tooth development

Although the morpho-, histo- and cytogenesis of the tooth have been well documented, the underlying biochemical signalling pathways controlling tooth development have not yet been fully elucidated. Currently, scientific studies are being conducted in an effort to determine genes and gene products that activate and regulate odontogenesis. These studies include specific processes in odontogenesis such as amelogenesis and/or dentinogenesis. Genes which have been identified as important in odontogenesis, especially during the cap and bell stage are, for example, *Dlx*-, *Msx*-, *Bmp*- and the *Notch* families (Mitsiadis *et al*., 1995; Cobourne, 1999; Stephanopoulos *et al*., 2005) including structural genes coding for amelogenin, amelotin, ameloblastin, enamelin, KLK-4 and enamelysin (Fukumoto *et al*., 2004; Iwasaki *et al*., 2005; Stephanopoulos *et al*., 2005;

Torres-Quintana *et al*., 2005). Various growth factors have also been identified which contribute to tooth development, such as epidermal growth factor (EGF) and fibroblast growth factor (FGF), which are essential for the initiation of tooth formation (Kronmiller *et al*., 1995a; 1995b; Cobourne and Sharpe, 2003). Retinoic acid (RA) has also been suggested as important in the initiation and patterning of odontogenesis (Kronmiller et al., 1995a). Amongst its functions, RA is said to promote the expression of different genes that are involved in terminal differentiation of specific cells (Mitsiadis *et al*., 1995; Kronmiller *et al*., 1995b; Berkovitz *et al*., 2001) such as ameloblasts.

1.2.1 Retinoic acid and tooth formation

Retinoic acid (RA), a derivative of retinol (vitamin A), is manufactured from the oxidative reaction when retinol is converted to RA via specific retinoic acid-synthesizing enzymes 1, 2, and 3 (Berkovitz *et al*., 2001; Niederreither *et al*., 2002). RA is able to associate with specific nuclear receptors (retinoic acid receptors) (Huq *et al*., 2007), which are transcription factors regulating a diverse number of genes. RA is also able to upregulate the production of the EGF receptor (Kronmiller *et al*., 1995a) and its ligand EGF, which are important initiation factors required for tooth development. Kronmiller *et al*. (1995a) showed that RA peaks early (at E11.5) in mice, the same stage during which dental lamina formation is initiated. They found that a loss of RA prevented correct dental lamina formation and normal tooth morphology. Furthermore, when exogenous RA was added *in vitro* to E11.5 embryonic mouse molars, the development of supernumary tooth buds occurred (Kronmiller *et al*., 1995a). RA is spatially distributed

from the region of the incisors (lowest) to the molars (highest) (Kronmiller *et al*., 1995a), thus forming a concentration gradient across the maxilla and mandible. It is this concentration gradient which is said to regulate the initiation of tooth development at particular time intervals during embryogenesis. RA was also found to upregulate *Notch* genes, which provided insight into how tissue patterning in the tooth could occur (Mitsiadis *et al*., 1995).

Notch was first isolated, analyzed and sequenced from *Drosophila melanogaster*, before a homologue was found in humans and mice. Its function is related to the pathway of determining cell fate (Mitsiadis *et al*., 1995). Coffman *et al.* (1993) postulated that the role of Notch is to block cell transformation by maintaining the competence of undifferentiated cells until such time as differentiation proceeds. RA has been linked to upregulating *Notch* expression which consequently appears to prevent cells from terminal differentiation. An example of this is during the formation of ameloblasts, where *Notch* is upregulated via RA until amelogenesis is to be initiated (Mitsiadis *et al*., 1995). During prenatal development RA levels drop to a specific concentration and *Notch* is downregulated (Mitsiadis *et al.*, 1995) allowing previously undifferentiated cells to change into ameloblasts.

1.2.2 Citral

Citral (3, 7-dimethyl-2, 6-octadienal) was found to be a competitive inhibitor of RA, retinal and retinol by Schuh *et al*. (1993). Kronmiller *et al*. (1995a) further demonstrated the suppressing effects of citral when they showed that it could inhibit retinoic acid

synthesis and thus prevent the initiation of odontogenesis, specifically dental lamina formation. In their experiments Kronmiller *et al.* (1995a) also revealed that citral was able to inhibit all-*trans-RA*, yet none of the *cis-RA* groups. Thus Kronmiller *et al.* (1995a) proved that at E11.5, inhibition of RA synthesis (all-*trans-RA*) resulted in altered patterning of the dental lamina. These same authors stated that an addition of 0.04µM of all-*trans-RA* to the growth medium was able to partially rescue tooth formation from initial citral inhibition. However, no research was performed to see how citral-induced inhibition of RA affected the later stages, such as the cap stage (E14) or bell stage (E16) of tooth development and how this impacted crown morphology as well as amelogenesis. There is evidence which shows that RA is still present in lesser quantities in neonatal day 5 mice in the region of the developing tooth, as the specific enzymes RALDH2 and 3 are still expressed long after the majority of the retinol had dissipated from the oral region (Niederreither *et al*., 2002). This indicates that there are still minor amounts of retinol present. Thus it is possible that RA still regulates genes after the bell stage, possibly even those of the *Notch* family, indicating a more specific role of RA in odontogenesis, other than just assisting in dental lamina formation and the initiation of tooth development.

1.2.3 PI3-kinase, laminins and wortmannin

Wortmannin, a naturally synthesized fungal metabolite derived from *Penicillium fumiculosum*, was used by Fukumoto *et al.* (2005) to show that phosphatidylinositol 3-kinase (PI3K) inhibition resulted in altered cusp morphology of the tooth when applied to E12.5 to 14.5 day embryonic teeth. Platelet derived growth factor regulates PI3K

activation (Pedigo *et al.*, 2007), which then controls laminin production via protein kinase B/Akt (Li *et al.*, 2001). Laminins consist of three genetically distinct α, β and γ chains. There are five α and three of each β and γ chains, which form 15 isoforms of laminin (laminin-1 to -15) with different sub-unit permutations (Fukumoto *et al.*, 2005). Laminins make up the majority of the basement membrane, which is composed of two layers, i.e. an internal basal lamina and an external fibrillar reticular lamina (Sanes, 2003). The external lamina is composed of fibrillar collagen whereas the basal lamina contains non-fibrillar collagen, together with non-collagenous glycoproteins, proteoglycans (Sanes, 2003) and laminins (Fukumoto *et al.*, 2005). It is believed that some of the proteins, i.e. the laminins in the basal lamina, are key regulators in causing cells to become polarized and to stimulate cytodifferentiation of ameloblasts and odontoblasts (Moss-Salentijn and Hendricks-Klyvert, 1990). Laminins accomplish this by binding with specific cell surface receptors including integrins, syndecans and α-dystroglycans, which regulate various biological activities including cell adhesion, migration, differentiation, angiogenesis and tumour metastasis (Fukumoto *et al*., 2005).

An important member of the laminin family is the laminin α5 chain which is expressed in many fetal and adult tissues. Associating either with laminin chain γ1 or β2, which are the main constituents of the basement membrane (Yurchenco *et al.*, 2004), to form laminin-10 or laminin-11, laminin α5 is able to regulate cell migration, nuclei polarity and cytodifferentiation of emerging cell lineages. When laminin α5 synthesis is perturbed via a PI3K/wortmannin interaction during mouse tooth development, cellular organization is lost and a malformation, such as altered cusp morphology, arises (Fukumoto *et al.*, 2005). However it is unclear whether the inhibition of PI3K affects

amelogenin mRNA expression during tooth development and how great the loss in laminin α5-mRNA levels must be to produce this alteration in cusp morphology.

2. Aim

The aim of this study was thus to investigate how amelogenesis and tooth morphology are affected during specific stages (cap and bell stage) of tooth development *in vitro*, when retinoic acid and PI3-kinase were inhibited by citral and wortmannin respectively. The first mandibular molar of the mouse was used as the model system for this experiment.

3. Materials and Methods

3.1 Animals used in the study

Animal ethics clearance for this experiment was obtained from the Animal Ethics Committee of the University of the Witwatersrand, Johannesburg, South Africa (Clearance Number 2006/17/01).

Sixteen female NMRI x NMRI pregnant mice and two 6.5 day mouse pups were used in this research. Of the pregnant animals, eight were 14.5 days pregnant and eight were 16.5 days pregnant. The rationale for using 14.5 and 16.5 day pregnant mice was that on these days the first mandibular molars of embryonic mice would have entered the cap and bell stages respectively. Furthermore, at these two stages various genes become active which are important for cytodifferentiation, histogenesis and morphogenesis of the developing tooth. Therefore, any changes in tooth development may be most pronounced, when citral or wortmannin are applied during these two prenatal ages.

Female NMRI x NMRI mice were mated with males of known fertility and the age of pregnancy was determined by the appearance of a vaginal plug on the morning following copulation. This was considered to be day 0.5 of pregnancy. At the appropriate age of pregnancy i.e. either 14.5 days or 16.5 days, the mouse was removed from the animal unit. Animals were killed by a lethal injection of 0.4ml of Euthanase (Kyron Laboratories, Johannesburg).

3.2 Tooth extraction

An incision was made in the abdominal region of each pregnant animal. The uterine horns containing the embryos were then removed and placed in a petri-dish in sterile Tyrode's solution (Appendix A) containing 1% glucose and 100UI/ml penicillin/streptomycin. The container with the uterine horns was then placed in an incubator at 37^{o}C.

Under sterile conditions an embryo was excised from a uterine horn and placed into a black wax dish containing Tyrode's solution (Fig. 2A). The murine embryos were then decapitated and the lower jaw was separated from the head (Fig. 2B and C). The lower jaw was then transferred on to a cavity block containing resin (Fig. 2D) and Tyrode's solution. Utilizing both incident and transmitted light, the first mandibular molars were removed from either side of the jaw by micro-dissection (Fig. 2E). Extracted molars were then relocated into a glass cavity block containing Tyrode's solution. This block was placed on to a 37^{o}C heating plate for a short period of time to maintain cellular viability while explants were accumulated.

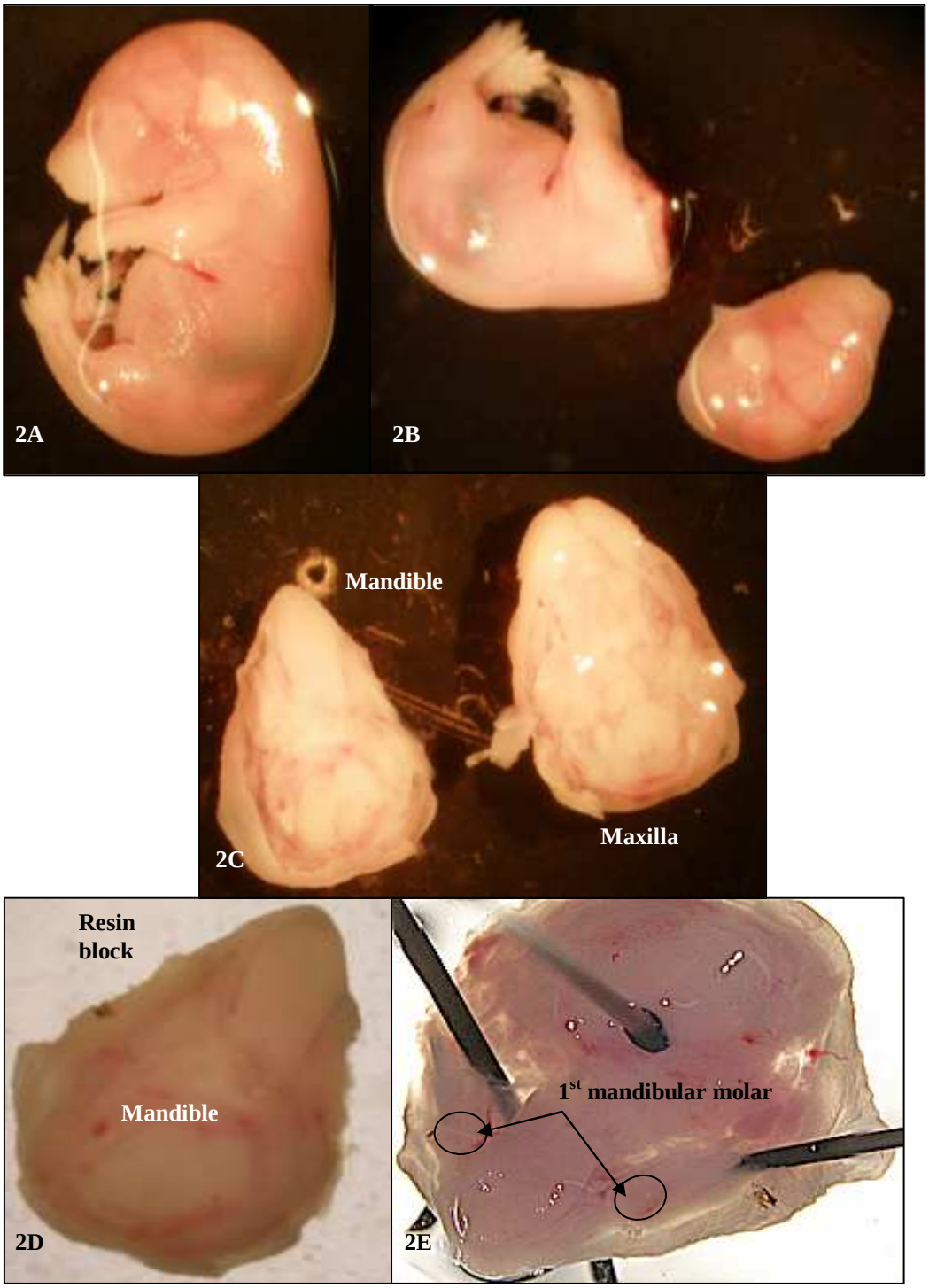

Figure 2. Photographic representation of micro-extraction procedure of first mandibular molars from 16.5 day old mouse embryos. The embryo was removed from the uterine horn and placed in a black wax dish (**A**) containing Tyrode's solution and then decapitated (**B**). The mandible and maxilla were separated from each other (**C**) and the mandible was transferred into a resin-containing cavity block (**D**).The first mandibular molars were then dissected free of the jaw (**E**). **Note: A-C** 25X stereomicroscope; D **and E** 40X stereomicroscope and transmitted light

3.3 Organ culture

Stainless steel rafts were placed into four-welled Nunc culture dishes (Microsep, Ireland). An Isopore membrane (Microsep, Ireland) manufactured at a pore size of 0.05 µm was then positioned on each stainless steel raft. To each well 800 to 900µl of BGjb culture medium (Modified Fitton and Jackson medium supplemented with L-glutamine, GIBCO, South Africa), supplemented with 10% fetal calf serum (FCS), 100µg/ml ascorbic acid and 100UI/ml pen/strep was added. For experimental explants, the culture medium was further augmented with either 1.75µM citral (Sigma-Aldrich, South Africa) or 20nM wortmannin (Sigma-Aldrich, South Africa), which are the optimal concentrations at which the inhibitors are said to operate (Kronmiller *et al*., 1995a; Stein and Waterfield, 2000). Three to four first mandibular molar explants were then placed onto each Isopore membrane. All explants were first cultured for a duration of 5-hours in a ThermoForma Series II water-jacketed CO_2 incubator (Labotec, South Africa) at 37^{o}C and an atmosphere of 5% CO_2 in air. The rationale for culturing explants for 5 hours in the presence of citral and wortmannin was to investigate whether changes in gene expression and cusp morphology could be altered in such a short time period as opposed to the reported exposure period of 24 hours (Kronmiller *et al.*1995a; Fukumoto *et* al. 2005). After the initial 5-hour treatment with BGjb medium containing either citral or wortmannin, the medium was substituted with fresh BGjb medium supplemented with 10% FCS, 100µg/ml ascorbic acid and 100UI/ml pen/strep. Explants were left to develop for 12 days at 37^{o}C at 5% CO_2 in air. The medium was changed every two days and explants were

examined for morphological variations with an Olympus inverted-phase contrast microscope. Photomicrographs were taken as necessary.

3.4 Histological analysis of tooth explants

3.4.1 Fixation of explants for sectioning

Thirty-six tooth explants (12 controls (14.5n=6; 16.5n=6), 12 citral-treated (14.5n=6; 16.5n=6) and 12 wortmannin-treated (14.5n=6; 16.5n=6)) were used for immunocytochemistry with two 6.5 postnatal mouse pup molars acting as positive controls. The remaining molar explants were utilized to analyze the general morphological and histological changes which may have occurred during the 12-day culture period and to compare the growth between control and treated molar explants. The teeth were recovered from the culture medium after 12 days and washed twice in 10% phosphate buffered saline (Appendix A). Explants were then fixed for 3 hours in 10 % buffered formalin (Appendix A), before being washed for 30 minutes in 10% PBS. The explants were then dehydrated through a graded series of alcohols, after which they were transferred into xylene for clearing for 10 minutes. Explants were then transferred into paraffin wax and left overnight. The following morning the explants were blocked in fresh paraffin wax.

3.4.2 Preparation of silane-coated glass slides

Slides were cleansed overnight in a 10% Extran solution. These were then washed for 2 hours under running tap water, before being left to dry in a 60^{o}C oven. Slides

were immersed in a 2% aminopropyltriethoxysilane (referred to as silane) solution for 30 minutes. They were then given two quick washes in acetone and one in distilled water. They were then allowed to dry in a 42^{o}C incubator overnight.

3.4.3 Immunocytochemistry

Serial sections of the fixed first mandibular molar tissue were cut at either 5 or 10µm on a Reichert-Jung Microtome and mounted on to silane-coated slides. Approximately 15-30 sections were obtained from each explant, depending on the thickness of the section. The sections were briefly dried on a Raymond[(a)] Lamb slide dryer, before being left in a 42^{o}C oven overnight. Sections were stored at room temperature until required.

Every fifth or tenth section from each explant was stained with haematoxylin and eosin (Appendix A) for routine histological examination. The indirect immunocytochemical method was used to localize amelogenin and laminin. Localization was carried out on sections adjacent to from those stained with haematoxylin and eosin which showed clear tissue definition.

For the localization of amelogenin and laminin, the sections were de-waxed in xylene and then hydrated through a graded series of alcohols to water. To block endogenous peroxidase, sections were incubated in 3% hydrogen peroxide for 10 minutes at room temperature. Following rinsing in 10% PBS, sections were incubated in 10% non-immune swine serum for 10 minutes at room temperature to

prevent non-specific binding of the antisera. Sections were then sequentially incubated with the primary antibody, rabbit anti-mouse amelogenin (1:200, Kamiya Biomedical, Washington) or rabbit anti-mouse laminin (1:25, Sigma, South Africa) at 4^{o}C overnight. Sections were then incubated with the secondary antibody (1:50 swine anti-rabbit, Dako, Denmark) for 1 hour at room temperature. Peroxide anti-peroxidase (PAP 1:100, Dako, Denmark) was then applied for 30 minutes, followed by a 5-minute incubation in diaminobenzide (DAB, BDH Laboratory Supplies, England) (Appendix A). Between the various incubations, sections were rinsed three times at 5 minutes each, in 10% PBS. All sections were viewed utilizing differential interference contrast microscopy (DIC) with the assistance of an Axioscope 2 Microscope which uses the computer-based program AxioVision Rel. 4.5. Being an optical microscopy illumination technique, DIC, also known as Nomarski optics is used to enhance the contrast in unstained, transparent samples such as those obtained by ICC.

3.4.4 Immunocytochemistry controls

The respective antiserum was applied to sections, which originated either from serial sections of cultured molars or from mouse pup first mandibular molars. Two different control procedures were carried out:

i) Negative controls were carried out on sections adjacent to those on which staining occurred, to test the specificity of the primary and secondary antisera. The primary (anti-amelogenin and anti-laminin) or secondary antiserum was replaced by 10% PBS or 1% swine serum. Replacing the

primary antiserum verifies that the immunolocalization is specific. Replacing the secondary antiserum, which carries the enzyme for the color substrate (DAB), confirms that there are no other endogenous enzymes reacting with the DAB.

ii) Positive controls were included in each immunocytochemical run to ensure the validity of the immunocytochemical technique itself. Sections from the first mandibular molar of a 6.5 day old NMRI mouse pup, known to be positive for the amelogenin antigen, and an adult mouse kidney (Animal Ethic clearance number 2006/17/01), known to be positive for the laminin antigen, were included in each run.

3.5 Amelogenin and laminin α5 gene expression in tooth explants

3.5.1 Primer design

Sequences of mouse amelogenin and laminin genes were researched on www.pubmed.com. Once an appropriate sequence had been found (~1kbp), forward and reverse primers were created (Table 1) to amplify a specific region within this sequence that was unique. This was determined by utilizing BLAST (www.pubmed.com) to cross-reference the primers to other sequences on the Pubmed databank. This ensured that the designated primers specifically amplified only the selected sequence. A second forward primer was also created that was localized within the first forward primer. In this way, a nested polymerase chain

Primer Name and direction	Primer sequence
Amelogenin Forward 1	TTTTGCTATGCCCCTACCAC
Amelogenin Forward 2	TACCACCTCATCCTGGAAGC
Amelogenin Reverse	ATGAGGCTGAAGGGTGTGAC
Laminin Forward 1	GTGGGGAGAGGGTACCTGAT
Laminin Reverse	TCTTGGGGGACACCTTGATA
B-actin Forward	TGATGGACTCCGGTGACGG
B-actin Reverse	TGTCACGCACGATTTCCCGC

reaction could be utilized, to increase the efficacy of amplification, by ensuring that only the sequence of choice was produced. Inqaba Biotech Laboratories, South Africa, then manufactured these sets of primers

Table 1. Primers for the amelogenin and the laminin gene

3.5.2 RNA extraction using the RNeasy ® Micro Kit

Thirty-six random tooth explants [12 controls (6x14.5 day; 6x16.5 day), 12 citral-treated (6x14.5 day; 6x16.5 day), 12 wortmannin-treated (6x14.5 day; 6x16.5 day)] were used for RNA extraction (RNeasy ® Micro kit Quiagen, South Africa), complementary DNA synthesis and subsequent PCR/Real-time PCR. On the day of the RNA extraction, explants were retrieved from the culture medium and washed in de-ionized water for 2 minutes. Each explant was then transferred into a QIA shredder Spin Column (Quiagen, South Africa). To assist with the lysis and homogenization of the tissue, 350µl of a β-mercaptaethanol/buffer RLT solution was added and microfuged for 3 minutes. The supernatant was transferred into a new 2ml

collection tube, to which 350µl of 70% ethanol was added to precipitate out DNA and cellular proteins. This mixture was immediately placed into RNeasy® MinElute Spin Column (Quiagen, South Africa) and centrifuged at maximum velocity for 15 seconds. The flow-through was discarded and 700 µl of buffer RW1 was added to denature all enzymes including RNase and DNase. Once this had been microfuged for 15 seconds, the 2ml collection tube was replaced and 500 µl of buffer RPE was added to the column for washing. After 15 seconds of microfugation, 500 µl of 80% ethanol was added to dry the column. This was then centrifuged for 2 minutes and both supernatant and the 2ml collection tube were discarded. The RNeasy® MinElute Spin Column was then transferred into a 1.5ml autoclaved eppendorf tube. The extracted RNA was then eluted by adding 50 - 100µl of RNase-free water to the column and microfuging for 2 minutes. The concentration and quality of the extract was measured by the use of a Nano-drop Spectrophotometer, Series ND-100. Samples were stored at -70^{o}C for further use.

3.5.3 cDNA synthesis using a Reverse Transcription PCR kit

Samples containing the extracted RNA from the first mandibular molar explants were taken from the -70^{o}C freezer and thawed on ice. Once the samples had liquefied, 1-5µl of RNA was added to 11µl of DEPL-treated water (Inqaba Biotech, South Africa) in a 0.5µl eppendorf tube. This was further augmented with 1µl of the oligod (T) primer (kit), tapped gently before being spun down, and left in a heating block set at 70^{o}C for 5 minutes, to denature any residual enzyme activity that could

interfere with the reverse transcriptase. The eppendorf tube was then placed back on ice and allowed to cool, after which 4µl 5x reaction buffer (kit), 2µl 10mM dNTP mix (kit) and 1µl Ribolock ribonuclease (kit) was added to the tube. The solution was incubated for 5 minutes at 37^{o}C to pre-heat the mix for the temperature-specific M-MulV reverse transcriptase (Inqaba Biotech, South Africa). The reverse transcriptase was then added immediately and the reaction was allowed to progress for 1 hour before being stopped by heating the solution to 70^{o}C in a heating block, which denatured the enzyme. The resulting complementary DNA was measured for both concentration and purity with the use of a Nano-drop Spectrophotometer Series ND-100, before being stored at -20^{o}C for further use.

3.5.4 Nested Polymerase Chain reaction

Nested PCR was performed to both optimize the primers and to identify amelogenin and laminin expression by amplifying the DNA of choice in the synthesized cDNA samples from the first mandibular molar explants. 2µl of cDNA was added to 8.5 µl DNase-free water to which 1µl of both forward primer 1 (amelogenin or laminin) and reverse primer (Table 1) was added. 12.5µl of GoTaq ® Green Master mix (Promega, South Africa) was included in this mix and the process was permitted to run for 30 cycles with a designated PCR machine program (see below) originating from Gibson, *et al.*, 2001.

Denaturation temperature	**94^{o}C**	**1 minutes**
Annealing temperature amelogenin primer	**61^{o}C**	**2 minutes**
Annealing temperature laminin primer	**59^{o}C**	**2 minutes**
Extension temperature	**72^{o}C**	**3 minutes**

The resulting solution was then diluted 20x in DNase-free water of which 10µl was added to a new 0.5ml eppendorf tube. A further 12.5 µl GoTaq ® Green Master mix (Promega, South Africa) was added and 1µl of forward primer 2 (amelogenin) or 1µl of forward primer 1 (laminin) (Table 1) and reverse primer was added. This sample was then amplified using the same PCR protocol.

An aliquot of 10µl of each amplified sample was then run on a standard 1.4% agarose gel supplemented with 10% ethidium bromide. In order to identify the amplified product a molecular weight marker (Appendix 1C) was also run on the gel. Fragments were visualized under a Pharmacia Image-Master VDS system (BIO-RAD, South Africa).

3.5.5 PCR controls

Two negative controls were included in each PCR run. The first was a water control containing forward and reverse primers but lacking the GoTaq ® Green Master mix (Promega, South Africa). This showed whether the water contained any DNA sequences that could be amplified during PCR. The second negative control

consisted of GoTaq ® Green Master mix (Promega, South Africa) with forward and reverse primers and lacking the DNase-free water. This indicated whether the GoTaq® Green Master mix (Promega, South Africa) was contaminated

The amplification of the β-actin gene represented the positive control and was included in each PCR run to test the viability of the synthesized cDNA and to ensure that the DNA originated from eukaryotic tissue.

3.5.6 Quantitative Real-time Polymerase Chain reaction

Quantitative Real-time PCR was performed with only the first set of primers, since the ABI 7500 PCR machine was able to detect low levels of amplification. The only substitution in the reaction mixture was that of the master mix, which was replaced by iTaq SYBR-green supermix (BIO-RAD, South Africa). The latter master mix is specifically designed to produce a fluorescent signal after each successful amplification of the designated substrate. With the help of the Applied Biosystems Software 7500 v1.2.3 and a PCR machine from Applied Biosystems, South Africa, coupled to a computer, both the relative quantity of the amelogenin and laminin α5 gene could be determined through the use of the C_t (threshold cycle) which was calculated by the software after each run. The C_t value was then converted to a numerical value using the following formula:

1.) $\Delta C_t = C_{t\,(sample)} - C_{t\,(endogenous\ control)}$

2.) $\Delta\Delta C_t = \Delta C_t - C_{t\,(Calibrator)}$

3.) $2^{-\Delta\Delta Ct}$ = relative quantity

Where

endogenous control = β actin

Calibrator = Amelogenin-or laminin α5 gene expression from 6.5 day mouse pup

In order to determine whether the gene expression was significant in control, citral-treated and wortmannin-treated groups, a paired Students' t-test was performed. Any t value ≥ t value at P = 0.05 was considered significantly different.

4. Results

4.1 Morphology and histology of the mouse first mandibular molar

Approximately 57% (n=140) of the NMRI x NMRI embryonic mouse first mandibular molar explants survived the 12-day culture period (Table 2), while the remaining 43% (n=104) degenerated or the explants keratinized. The teeth which survived the long culture period showed an increase in size of the molar bud, including clear morphodifferentiation of the molar into its typical multicuspid structure (Fig. 3).

Table 2. The percentage of molar explants in culture which survived

Age in days and type of treatment	Total teeth in culture	Number (and percentage) of cultured molar explants degraded or keratinized after 12 day culture	Number (and percentage) of cultured molar explants with normal development after 12 day culture
14.5 Control	42	16 (38.0%)	26 (61.9%)
14.5 Citral	18	6 (33.3%)	12 (66.7%)
14.5 Wortmannin	23	10 (43.5%)	13 (56.5%)
16.5 Control	79	38 (48.1%)	41 (51.9%)
16.5 Citral	45	18 (40.0%)	27 (60.0%)
16.5 Wortmannin	37	16 (43.2%)	21 (56.8%)
Total	244	104 (42.6%)	140 (57.4%)

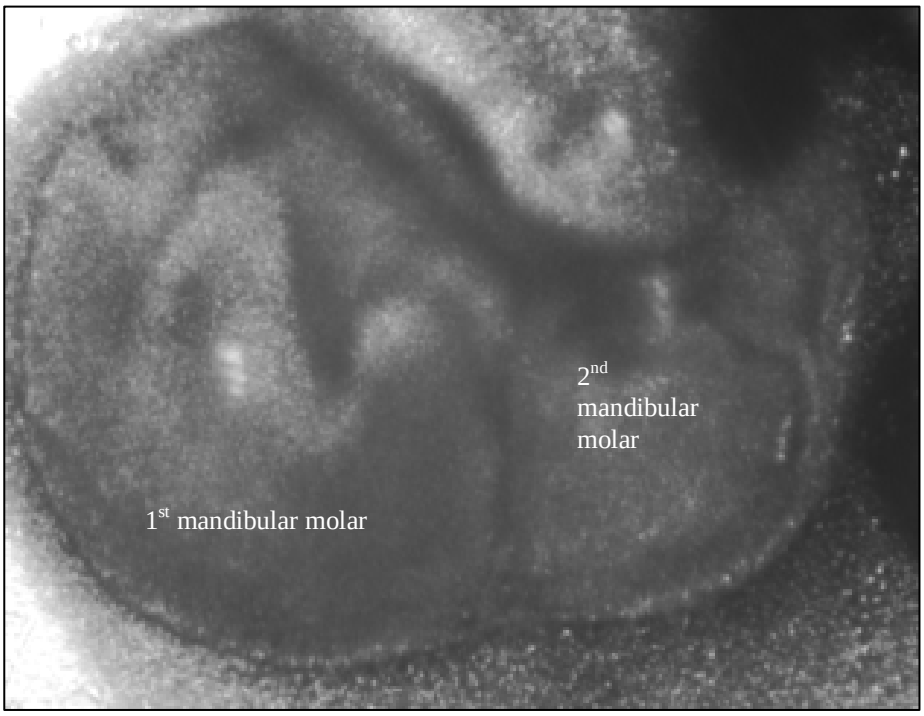

Figure 3. Representative photomicrograph of a multicuspid first and developing second mandibular molar after a culture period of 12 days.
10X stereomicroscope

Histological observations of 6.5 day mouse pup first mandibular molars

First mandibular molars (n=2) extracted from postnatal 6.5 day old mouse pups, showed that the teeth were at the late bell stage of tooth development. The stellate reticulum between the inner and outer enamel epithelial cells layers was clearly visible and the cells located on the surface of the differentiated ameloblasts had condensed into a thin cell layer, the stratum intermedium (Fig. 4A). The ameloblasts, stellate reticulum and stratum intermedium were distinguishable from each other, as there was no compression between these cellular layers. The ameloblasts had a columnar shape and their nuclei were

positioned at the basal pole of the cells (towards the stratum intermedium). Thick layers of enamel, dentin and predentin matrices could be observed, as well as columnar odontoblasts, which had differentiated from the underlying peripheral cells of the dental papilla (Fig. 4A). The dental follicle, a condensation of ectomesenchymal cells, surrounded the tooth bud.

Histological observations of 14.5 day and 16.5 day *in vitro* control first mouse molar explants

Control 14.5 day (n=26) and 16.5 day (n=41) embryonic first mouse molars, cultured for 12 days, showed that the teeth were at the early bell stage of tooth development (Fig. 4B = 14.5 day control molar; Fig. 4C = 16.5 day control molar). The epithelial cells, between the inner and outer enamel epithelial layers, had formed the stellate reticulum (Figs. 4B, 4C). The cells of the stellate reticulum had condensed and formed a thin stratum intermedium layer. The outer enamel epithelial layer, although present, was difficult to distinguish from the stellate reticulum or the stratum intermedium due to condensation between these cellular layers (not shown in Figs. 4B, C). The inner enamel epithelial cells (ameloblasts) were columnar in shape and their nuclei were at the basal pole of the cells. The enamel/dentin layers were absent and only a predentin layer was observed. The peripheral cells of the dental papilla, near the predentin layer had differentiated into odontoblasts (Fig. 4B), which were columnar in shape with their nuclei positioned at the basal pole of these cells. The cultured molar explants had a partially intact dental follicle,

which was found surrounding the tooth bud. There were no histological differences between the 14.5 day and 16.5 day control molar explants.

Histological observations of 14.5 day and 16.5 day citral-treated first mouse molar explants

Cultured 14.5 day (n=12) and 16.5 day (n=27) embryonic first mouse molars treated with citral for 5-hours, were also at the early bell stage of tooth development, following 12 days culture *in vitro*. The cells of the stellate reticulum had condensed and formed the stratum intermedium against the ameloblast layer (Figs. 4D, E). The outer enamel epithelium was observed in the molar explants (not shown in Figs. 4D, E) but, due to the high degree of condensation of the stratum intermedium and stellate reticulum near the outer enamel epithelium, it was very difficult to distinguish the various cellular layers. The ameloblasts were columnar in shape and their nuclei were situated at the basal pole of the cells, i.e. away from the original basement membrane (Fig. 4D, E). Neither an enamel nor dentin matrix was observed. However there was a very thick predentin layer. The underlying peripheral cells of the dental papilla, near the predentin border, had differentiated into odontoblasts. The dental follicle surrounding the tooth bud was present. There were no histological differences between 14.5 day and 16.5 day citral-treated molar explants. No histological variation could be observed when the 14.5 day and 16.5 day citral-treated molar explants were compared with the untreated cultured 14.5 day and 16.5 day molars.

Histological observations of 14.5 day and 16.5 day wortmannin-treated first mouse molar explants

There was little histological difference between molar explants cultured in citral or in wortmannin. The cultured 14.5 day (n=13) and 16.5 day (n=21) wortmannin-treated embryonic mouse first molars cultured for 12 days, showed that the teeth were at the early bell stage of tooth development. A stellate reticulum and stratum intermedium were present (Figs. 4F, G). The outer enamel epithelium was present in most of the molar explants but was once again condensed against the stellate reticulum. Columnar ameloblasts lined the undersurface of the "bell". No enamel or dentin matrix could be seen, but, there was a very thick predentin layer present, as seen in the citral-treated explants. The dental papilla was present and the cells bordering the predentin had differentiated into odontoblasts. There was no histological difference between the 14.5 day and the 16.5 day wortmannin-treated molar explants. When compared to the 14.5 day and 16.5 day control cultured molar explants, no deformities in either tooth cusp or tooth shape (not shown) or histology were observed in either the 14.5 day or the 16.5 day wortmannin-treated molar explants.

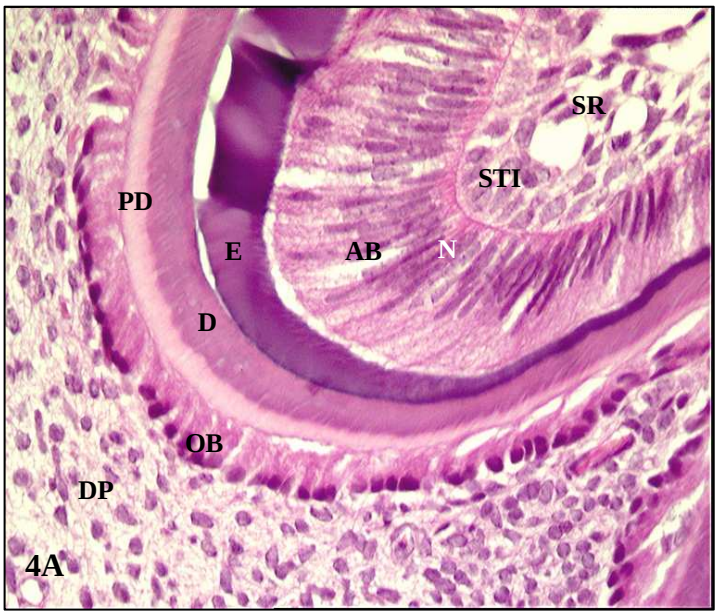
SR
STI
PD
E
AB
N
D
OB
DP
4A

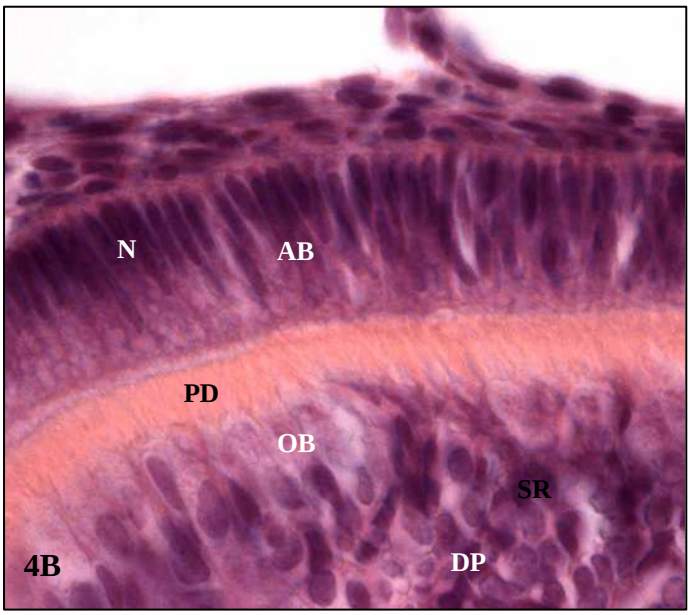
N
AB
PD
OB
SR
DP
4B

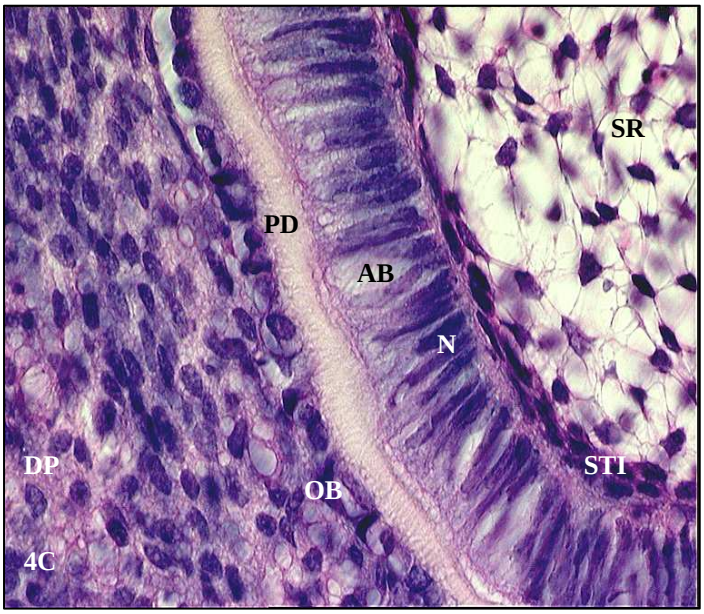
SR
PD
AB
N
DP
OB
STI
4C

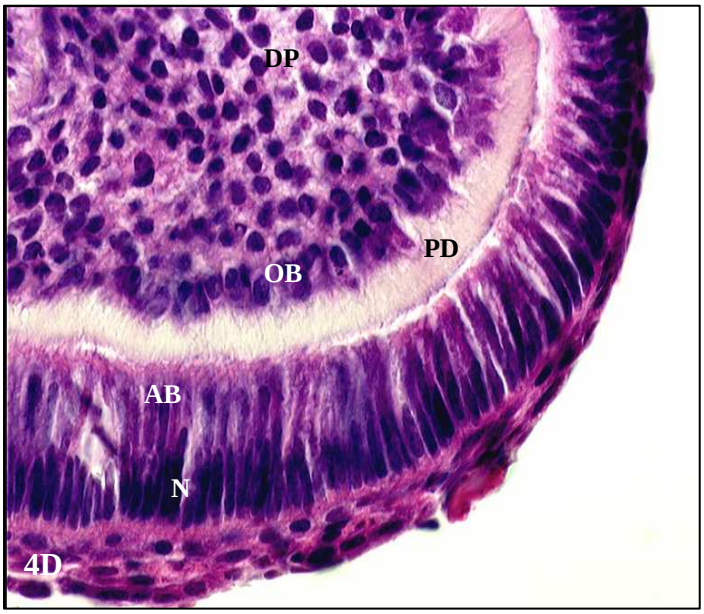
DP
PD
OB
AB
N
4D

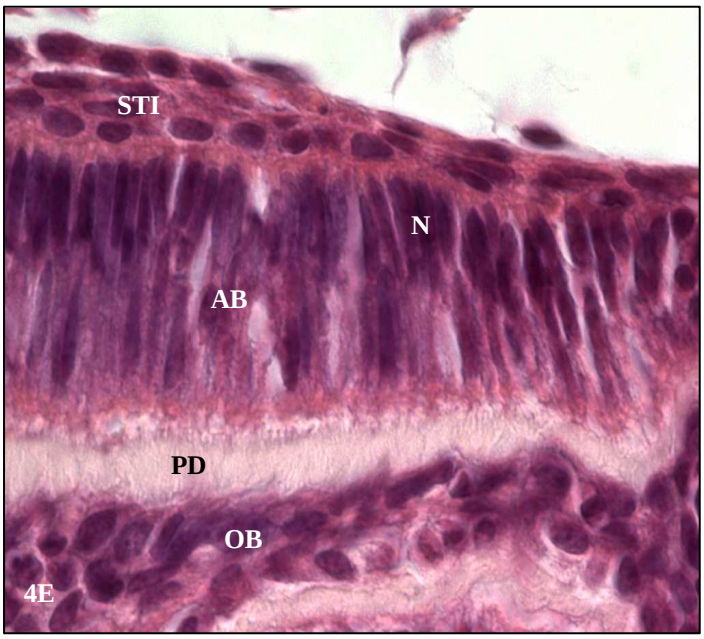
STI
N
AB
PD
OB
4E

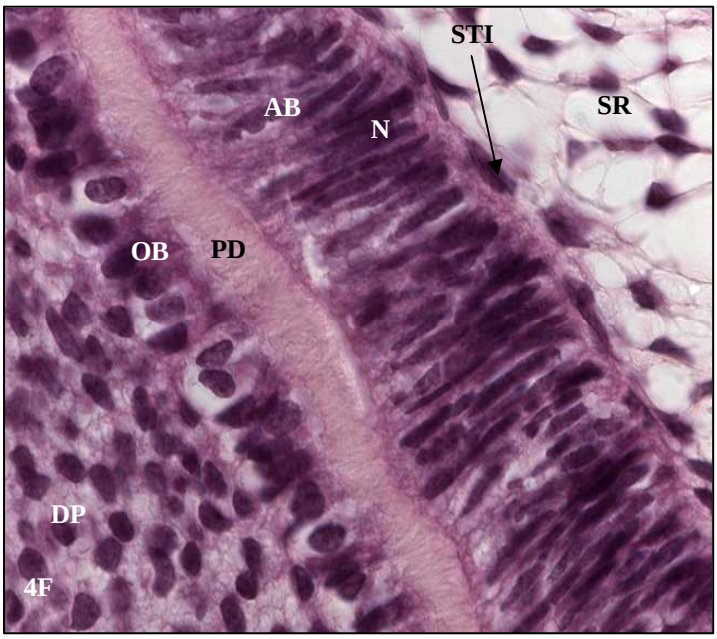
STI
AB
N
SR
OB
PD
DP
4F

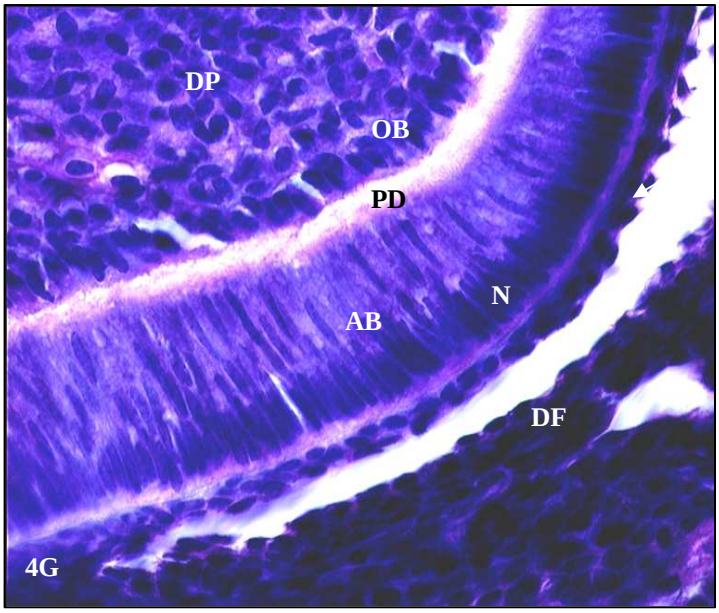

Figure 4. (**A**) Representative histological section of a first mandibular molar extracted from a 6.5 day mouse pup, to show specific cell and tissue layers of the tooth when the tooth is in the late bell stage of tooth development (63 X Light microscope (LM)). (**B**) Section from a 14.5 day embryonic first mandibular molar control explant, cultured for 12 days, showing the tooth at an early bell stage of tooth development. Note clear differentiation of ameloblast/odontoblast cells (100X LM). (**C**) Section of a control first mandibular molar from a 16.5 day mouse embryo, cultured for 12 days, at the early bell stage of tooth development (63X LM). (**D**) A section from a 14.5 day citral-treated embryonic mouse molar, cultured for 12 days, at the early bell stage of tooth development (63X LM). (**E**) A section taken from a 16.5 day mouse citral-treated embryonic mouse molar explant, cultured for 12 days, at the early bell stage of tooth development. Ameloblasts and odontoblasts have differentiated (100X LM). (**F**) Section from a 14.5 day, 12 day cultured first mandibular embryonic molar explant treated with wortmannin shows that the tooth is at the early bell stage of tooth development since ameloblast and odontoblasts have differentiated (100X LM). (**G**) A section of a 16.5 day embryonic mouse first mandibular molar cultured for 12 days and treated with wortmannin for 5-hours (63X LM). The molar is at the early bell stage of tooth development. Due to the obliqueness of the section it appears that the predentin is thicker than in the controls

Note: AB = ameloblasts; **OB =** odontoblast; **E=** enamel; **PD=** predentin; **D** = dentin; **DP** = dental papilla; **STI** = stratum intermedium; **DF** = dental follicle; **OEE** = outer enamel epithelium; **N** = nucleus

4.2 Immunocytochemistry

4.2.1 Amelogenin localization

6.5 day neonatal mouse molars

Both of the 6.5 day neonatal mouse pup first mandibular molars showed a positive immunoreaction for amelogenin. The immunolocalization of amelogenin, in the mouse pup molars was situated in the ameloblasts (Fig. 5A). Furthermore, amelogenin was found in the odontoblasts and their odontoblastic processes, which were observed as dark lines within the dentin matrix. Some immunolocalization was also observed in the stratum intermedium. One could argue that, the immunolocalization in the odontoblasts, odontoblastic processes and stratum intermedium are due to entrapment of air, but this is negated by the negative control. In negative controls (adjacent sections), no immunoreaction with the amelogenin antibody was obtained when either the primary or secondary antibody were replaced with non-immune rabbit serum (not shown) or PBS (Fig. 5B) respectively. However, in some instances the enamel reacted positively in the negative controls. This may be due to folds in the enamel between which DAB has become trapped and due to an over-exposure to light changed colour (Fig. 5B)

14.5 day and 16.5 day control molar explants

Of the six 14.5 day and the six 16.5 day control molar explants used to test for immunolocalization of amelogenin, three molar explants from each age group reacted positively with the anti-amelogenin antibody (Table 3). The immunolocalization for amelogenin was localized within the secretory tip of the ameloblast cells, where the Tomes process is located (Fig. 5C, 5D). Substitution of either the primary or secondary antibody in an adjacent section with non-immune rabbit serum or PBS respectively, produced negative results, i.e. no immunoreaction occurred (Fig. 5E**,** 5F). The immunoreaction in Fig. 5E is a photosensitive reaction that occurs when DAB becomes trapped in folds of the enamel, which is brought about due to uneven section cutting. No difference in amelogenin immunolocalization was observed when 14.5 day and 16.5 day control molar explants when compared with each other or when compared to the 6.5 day old mouse pup.

.

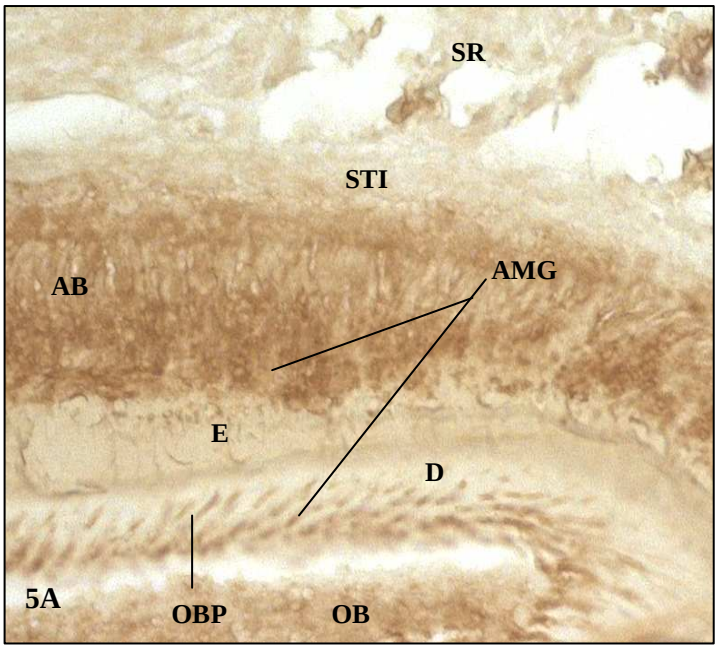
SR
STI
AB
AMG
E
D
5A
OBP
OB

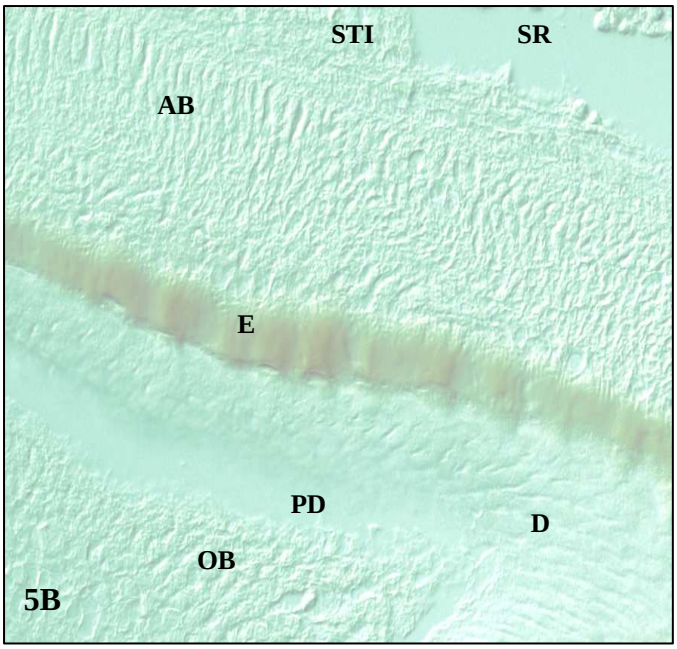
STI
SR
AB
E
PD
D
OB
5B

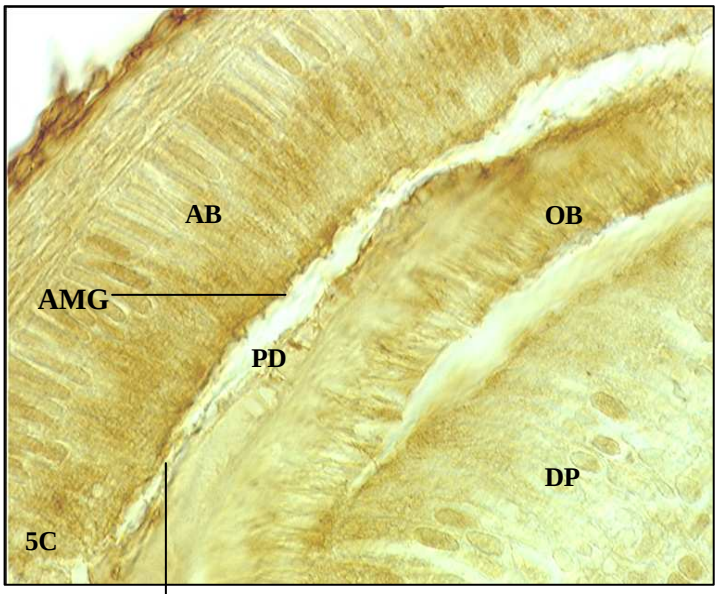
AB
OB
AMG
PD
DP
5C
TP

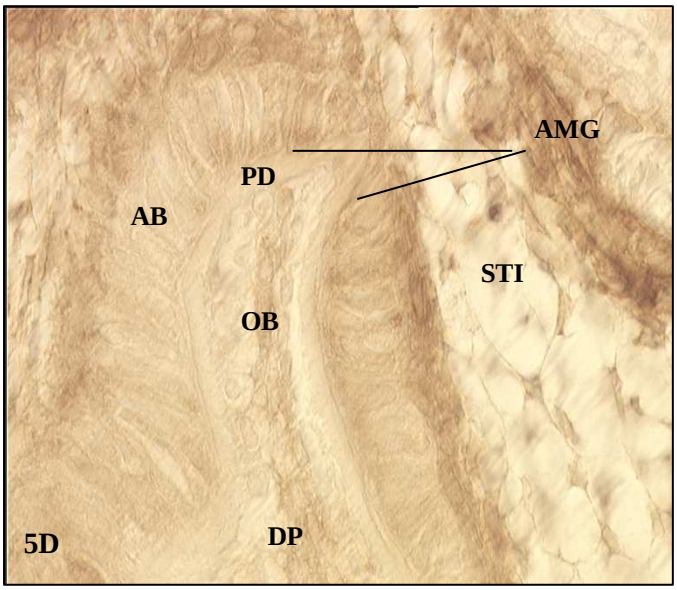
AMG
PD
AB
STI
OB
DP
5D

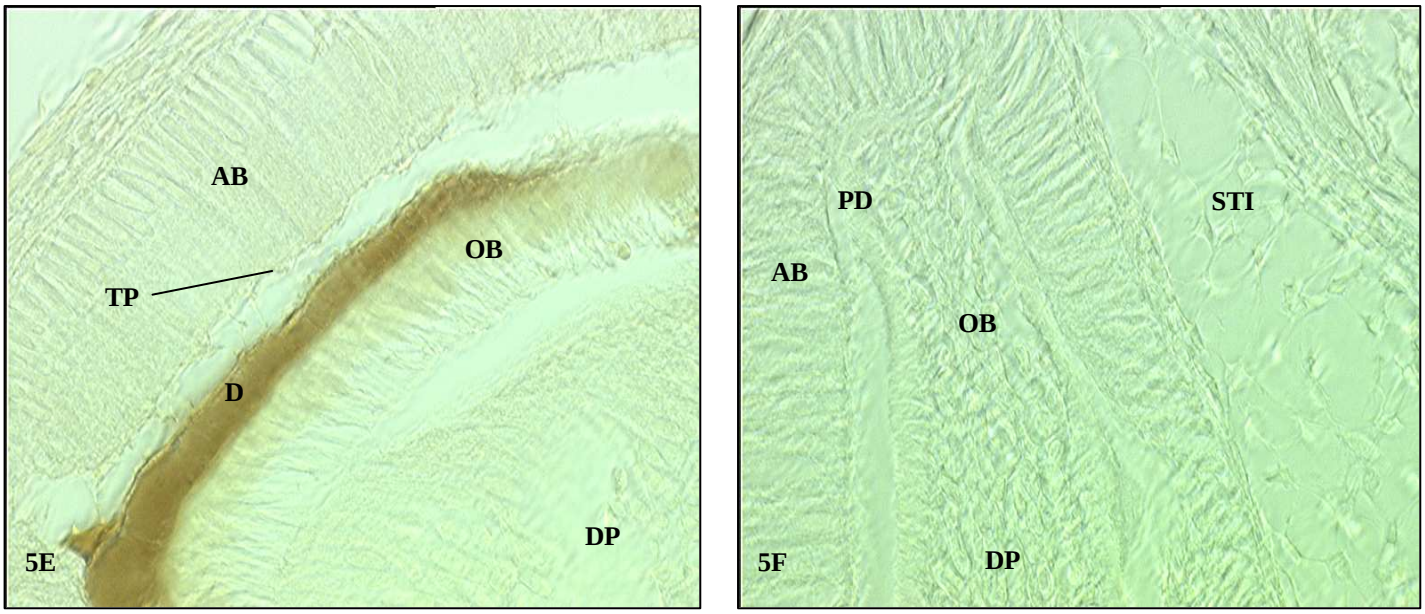

Figure 5. (**A**) Representative photomicrograph of a 6.5 day neonatal mouse pup first mandibular molar in which amelogenin immunolocalization has occurred in ameloblasts, odontoblasts, odontoblastic processes and stratum intermedium (100X Differential interference contrast microscope (DIC). (**B**) Negative control of a 6.5 day mouse pup molar shows no amelogenin localization when secondary antibody is replaced with PBS. Note DAB which has become trapped in folds in the enamel is reacting due to an over-exposure to light and is not to be confused with immunolocalization (100X DIC). (**C**) Representative photomicrograph of a 14.5 day cultured control embryonic mouse molar immunolocalized for amelogenin, shows localization in the secretory pole of the ameloblast cells including the Tomes process located at the tip of the secretory cell surface of the ameloblasts (63X DIC). (**D**) Representative photomicrograph of a 16.5 day cultured control embryonic mouse molar, immunolocalized for amelogenin shows clear localization in the ameloblast cells including a thin line running along the tip of the ameloblasts/predentin border (63X DIC). (**E)** Substitution of the primary antibody with non-immune rabbit serum shows no localization to be present when tested in an adjacent section to the section (Fig. 5C) used for positive immunolocalization (63X DIC). The darkening in the section is due to the same effect described in Fig. 5B. (**F**) Negative control section, adjacent to the section used for positive immunolocalization (Fig. 5D) in which the secondary antibody was substituted with PBS shows no localization for amelogenin (63X DIC).

Note: AB = ameloblast; **OB** = odontoblast; **PD** = predentin; **DP** = dental papilla; **STI** = stratum intermedium; **TP** = Tomes process; **AMG =** amelogenin; **D** = dentin; **E** = enamel; **SR** = stellate reticulum. (**B**) is an adjacent section to (**A**); (**E**) is an adjacent section to (**C**); (**F**) is an adjacent section to (**D**)

Table 3. The number of explants from the various groups which reacted positively with the amelogenin or laminin antibody.

Age and type of molar explant	Number of explants used for ICC	Number (and percentage) of cultured molar explants with amelogenin immuno-localization	Number (and percentage) of cultured molar explants with no amelogenin immuno-localization	Number (and percentage) of cultured molar explants with laminin immuno-localization	Number (and percentage) of cultured molar explants with no laminin immuno-localization
14.5 Control	6	3 (50.0%)	3 (50.0%)	2 (33.3%)	4 (66.6%)
14.5 Citral	6	3 (50.0%)	3 (50.0%)	2 (33.3%)	4 (66.6%)
14.5 Wortmannin	6	2 (33.3%)	4 (66.6%)	2 (33.3%)	4 (66.6%)
16.5 Control	6	3 (50.0%)	3 (50.0%)	4 (66.6%)	2 (33.3%)
16.5 Citral	6	2 (33.3%)	4 (66.6%)	3 (50.0%)	3 (50.0%)
16.5 Wortmannin	6	3 (50.0%)	3 (50.0%)	4 (66.6%)	2 (33.3%)
Total	36	16 (44.4%)	20 (55.6%)	17 (47.2%)	19 (52.8%)

14.5 day and 16.5 day citral-treated first molar explants

Of the six 14.5 day and the six 16.5 day citral-treated molar explants, three 14.5 day and two 16.5 day molar explants showed positive immunolocalization for amelogenin (Table 3). The amelogenin peptide was localized in the secretory tip of the ameloblasts, where the Tomes process originates, as well as in some of the odontoblasts (Fig. 6A, 6B). Furthermore, during the sectioning of some of the explants an artifactual break occurred in the tissues, which led to some ameloblasts being separated at the ameloblast/predentin junctions. The effect of this was that some immunolocalization occurred on the surface of the predentin matrix, in fragments of the Tomes process left behind during the ameloblast separation. When 14.5 day and 16.5 day citral-treated molar explants were either compared to

each other or to the 14.5 day and 16.5 day cultured control molar explants no difference in amelogenin immunolocalization was observed.

14.5 day and 16.5 day wortmannin-treated first molar explants

Of the six 14.5 day and the six 16.5 day wortmannin-treated first molar explants, two 14.5 day and three 16.5 day molar explants showed positive immunolocalization for the amelogenin peptide (Table 3). The immunolocalization was observed in the apical tips of the odontoblasts and in the Tomes processes of the ameloblasts (Fig. 6C, 6D). No difference in immunolocalization was detected between 14.5 and 16.5 day wortmannin-treated molar explants. In relation to the untreated cultured 14.5 day and 16.5 day molar explants no difference in immunolocalization was observed.

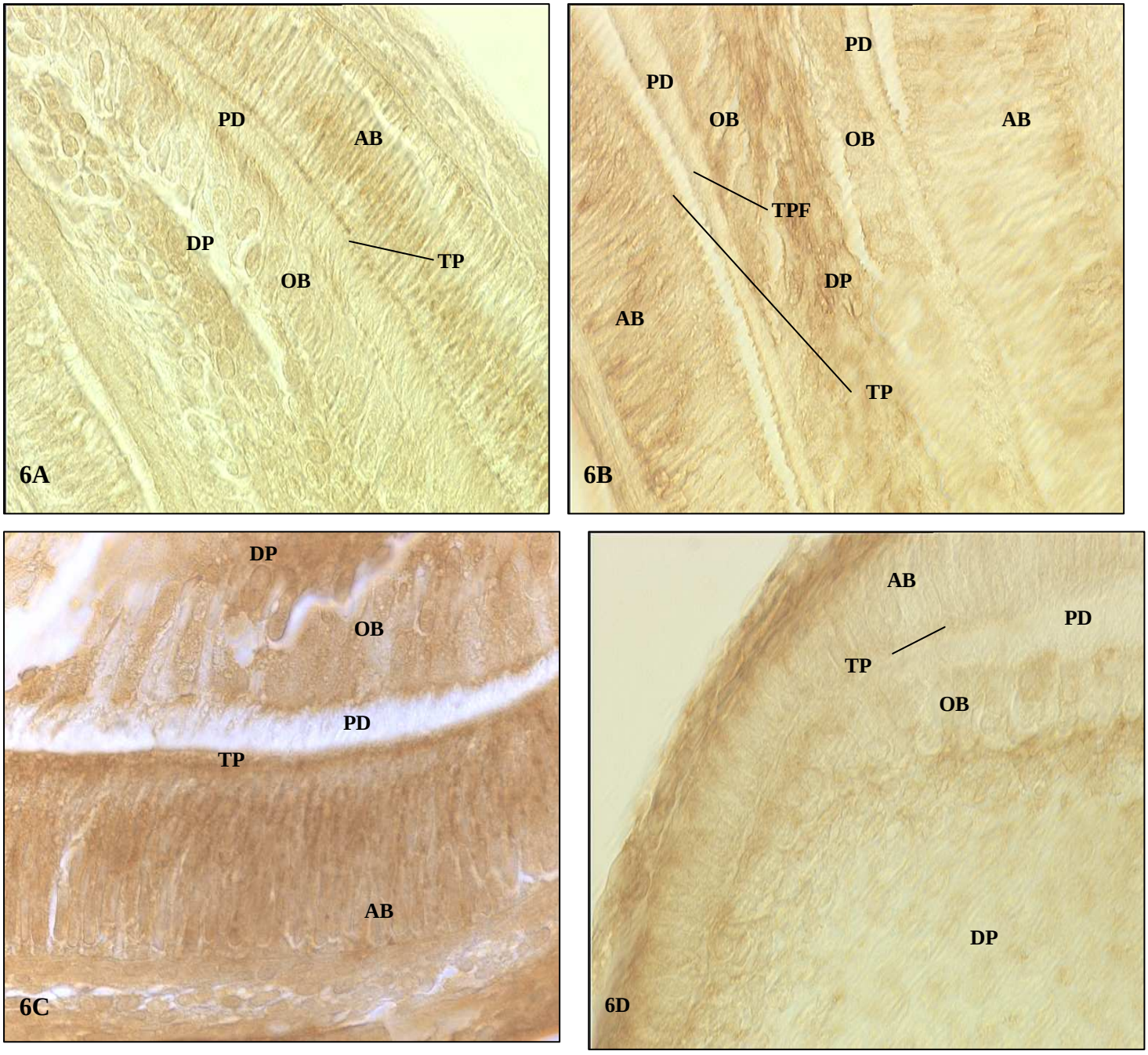

Figure 6. (**A**) Representative photomicrograph of a section from a 14.5 day citral-treated first mandibular molar explant (63X DIC) amelogenin shows that the peptide is localized near the secretory tip of the ameloblast cells, where the Tomes process is located. (**B**) In a section from a 16.5 day citral-treated molar explant (63X DIC) immunolocalized for amelogenin, the protein is localized at the secretory poles of the ameloblast cells, where the Tomes process is found. (**C**) Positive immunolocalization for amelogenin was also seen in the section of a 14.5 day molar (100X DIC) and (**D**) 16.5 day molar explant (63X DIC) which were treated for 5-hours with wortmannin. Amelogenin was found to be immunolocalized near and around the Tomes process of the ameloblast and in the secretory tips of the odontoblasts.

Note: AB = Ameloblasts; **OB =** Odontoblasts; **PD** = dentin; **TP** = Tomes Process; **DP** = dental papilla; **TPF** = Tomes Process fragments

4.2.2. Laminin immunolocalization

6.5 day neonatal first mouse molars

A positive immunoreaction for the laminin antibody was observed in both of the 6.5 day mouse pup first mandibular molars utilized. The laminin peptide was immunolocalized at the basal end of the ameloblasts (Fig. 7A). Interestingly the enamel matrix also showed immunolocalization for laminin. However, this was determined to be an artifactual reaction which is caused when, during sectioning of the tissue, folds are created in the inorganic matrix, i.e. enamel. The grooves produced by enamel can trap excess dye i.e. DAB, which due to its photosensitivity reacts over time, giving the impression that the inorganic matrix reacted. The negative control sections clearly showed this phenomenon. There was no immunolocalization in the other tissue layers of the molar when either the primary or secondary antibodies were replaced with non-immune rabbit serum or PBS (Fig. 7B) respectively, except in the enamel matrix.

14.5 day and 16.5 day control molar explants

Of the six 14.5 day and the six 16.5 day control molar explants used to immunolocalize laminin, two 14.5 day and four 16.5 day molar explants reacted positively with the anti-laminin antibody (Table 3). No immunoreaction for laminin occurred in the secretory poles of either the ameloblasts or the odontoblasts of the control molar explants (Fig. 7C, 7D). However, there was immunolocalization of

laminin between the ameloblasts and odontoblasts, which appeared to be a residual basement membrane. This immunolocalization was seen in both the 14.5 day and 16.5 day control molar explants (Fig. 7C, D). When either the primary or secondary antibody was substituted with non-immune rabbit serum or PBS respectively, no immunolocalization for laminin occurred (Fig. 7E, 7F). Compared to each other, 14.5 and 16.5 day control molar explants showed no difference in terms of laminin immunolocalization. However compared to the 6.5 day mouse pup molar immunolocalization, 14.5 day and 16.5 day molar explants did not show laminin immunolocalization in the basal region of the ameloblasts.

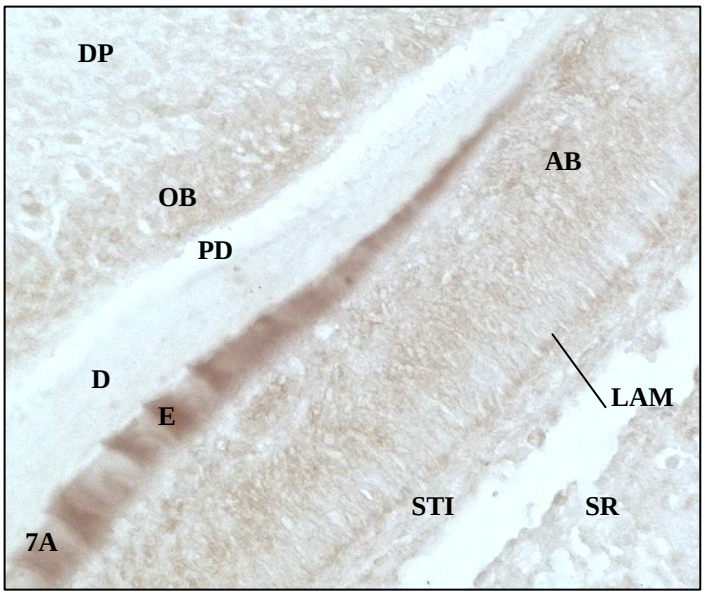
DP
AB
OB
PD
D
E
LAM
STI
SR
7A

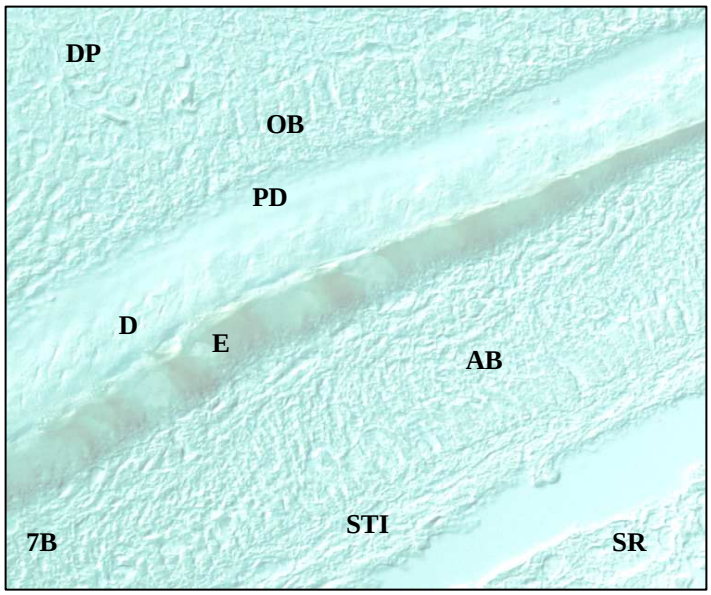
DP
OB
PD
D
E
AB
STI
SR
7B

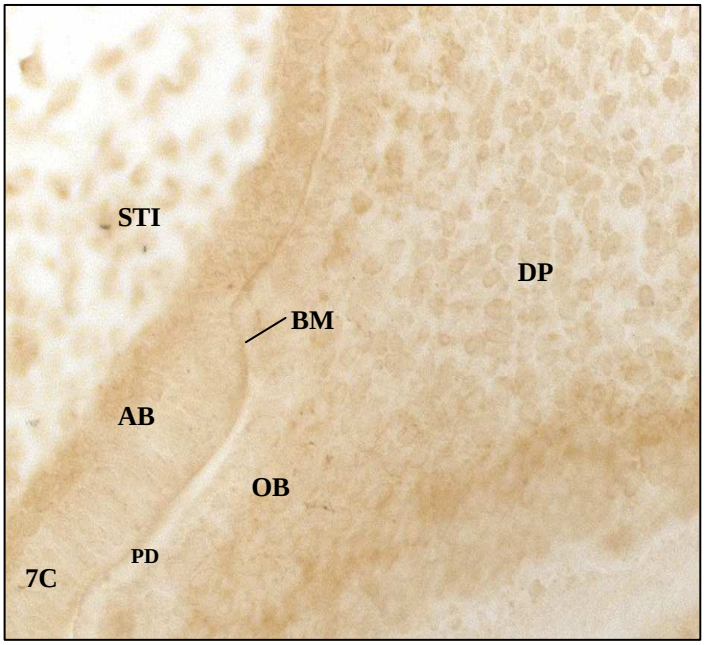
STI
DP
BM
AB
OB
PD
7C

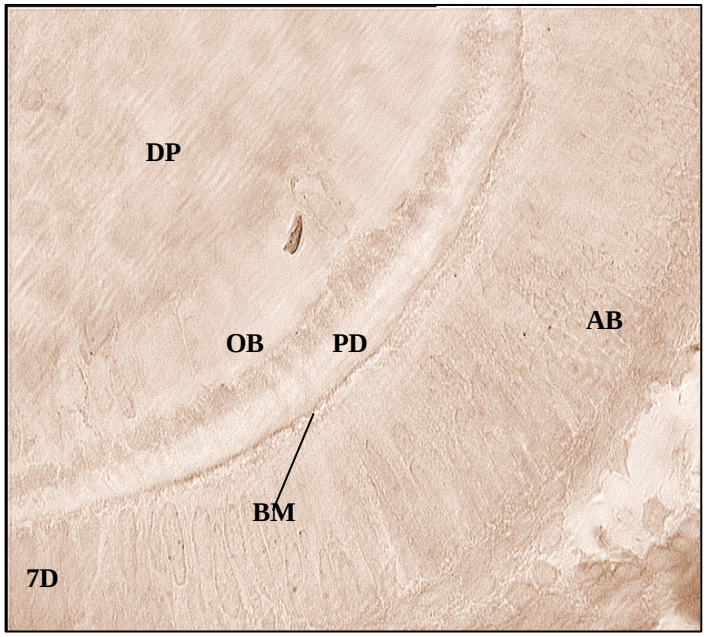
DP
AB
OB
PD
BM
7D

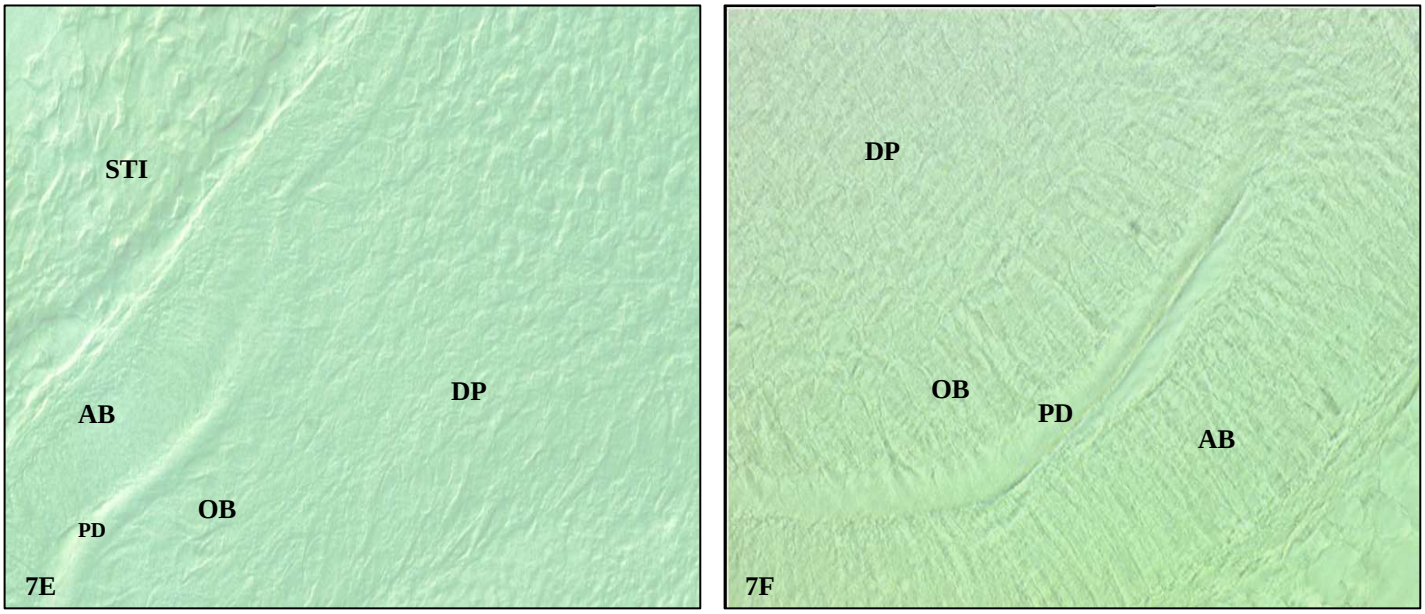

Figure 7. (**A**) Representative photomicrograph of a neonatal first mandibular mouse pup molar for the immunolocalization of laminin. (63X DIC) (**B**) Replacing the secondary antibody with PBS, in an adjacent section, showed no localization of laminin. Note that the DAB is reacting with the calcium ions in the enamel matrix which is not to be confused with immunolocalization (63X DIC). Therefore the localization seen in Fig. 7A in the enamel matrix is an artifactual reaction. (**C**) Representative photomicrograph of a 14.5 day cultured first mandibular control molar, indicating immunolocalization for laminin in the basement membrane region (63X DIC) (**D**) Representative photomicrograph of a 16.5 day cultured first mandibular control molar, shows that laminin immunolocalization occurred at the ameloblast/predentin junctions (63X DIC). (**E**) In an adjacent section in which the primary antibody was replaced with non-immune rabbit serum there is no immunolocalization of laminin (63X DIC) (**F**) Substitution of the secondary antibody with PBS, in an adjacent section to the one used in Fig.7D, did not produce a reaction (63X DIC)

Note: AB = ameloblasts; **OB** = odontoblasts; **PD =** predentin**; STI** = stratum intermedium; **BM** = basement membrane; **D** = dentin; **PD** = dental papilla; **E** = enamel; **SR** = stellate reticulum; **LAM** = laminin. (**B**) is an adjacent section to (**A**); (**E**) is an adjacent section to (**C**); (**F**) is and adjacent section to (**D**)

14.5 day and 16.5 day citral-treated first molar explants

Of the six 14.5 day and the six 16.5 day citral-treated first molar explants tested for laminin immunolocalization, two 14.5 day and three 16.5 day molar explants reacted weakly with the laminin antibody (Table 3). Once again, the immunolocalization for laminin was observed between the ameloblast layer and the predentin and was found either near the cusps of the 14.5 day citral-treated molar explants (Fig. 8A) or near the cervical loop of the 16.5 day citral-treated molar explants (Fig. 8B). Neither the ameloblasts nor the odontoblasts showed any immunolocalization for laminin. When compared to the 14.5 day and 16.5 day control molar explants, no difference in laminin immunolocalization was observed in those explants treated with citral.

14.5 day and 16.5 day wortmannin-treated molar explants

Of the six 14.5 day and the six 16.5 day wortmannin-treated molar explants, two 14.5 day and four 16.5 day molars showed positive immunoreactivity with the laminin antibody (Table 3). In the 14.5 day wortmannin-treated molars (Fig. 8C, circled area) there was weak immunolocalization, in the region where the basement membrane is normally situated. The odontoblasts did not show any localization for laminin. In the 16.5 day wortmannin-treated molars (Fig. 8D) immunolocalization was predominantly observed in the apical tips of the ameloblasts. It would seem that laminin localization was also found in the stratum intermedium but this immunolocalization occurred because stellate reticulum and stratum intermedium

were highly condensed. When comparing the 14.5 day and 16.5 day wortmannin-treated molars to the 14.5 day and 16.5 day untreated molar explants, the main difference was that the wortmannin-treated explants showed laminin immunolocalization in the apical tips of the ameloblasts but lacked the laminin localization between the ameloblasts and odontoblasts cell layers.

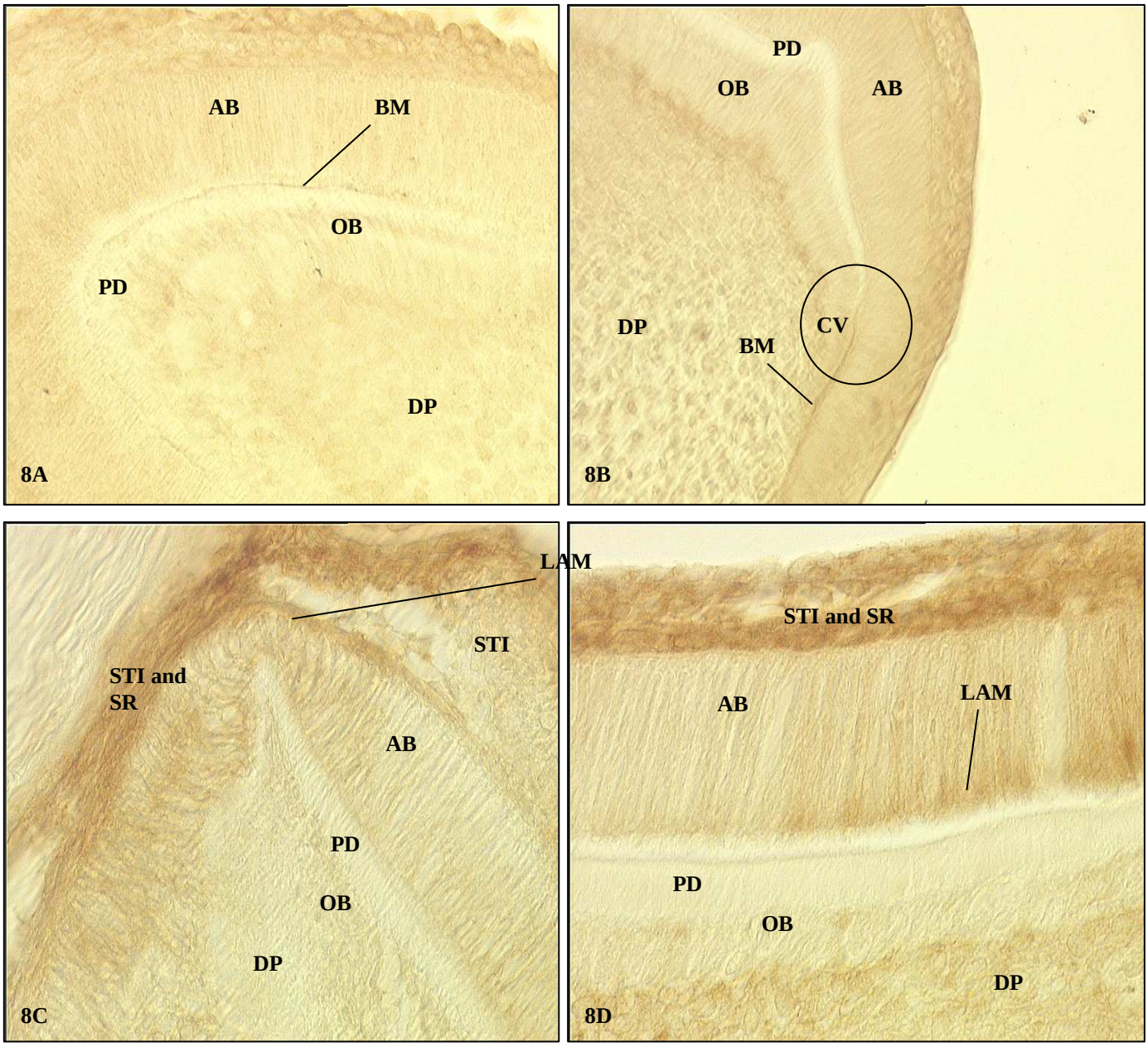

Figure 8. (**A)** Representative photomicrograph of a 14.5 day citral-treated first mandibular molar explant section, showed immunolocalization at the tip of the cusp of the molar, between the ameloblasts and predentin (X63 DIC). (**B**) Representative photomicrograph of a 16.5 day citral-treated first mandibular molar explant section showed immunolocalization of laminin to be present only in the basement membrane near the cervical region of the root of the tooth (X63 DIC). (**C**) A section of a 14.5 day molar explant which was treated for 5-hour s with wortmannin, showed immunolocalization of laminin in the basal tip of the ameloblast (X63 DIC). (**D**) In the section of a 16.5 day wortmannin-treated first mandibular molar explant laminin immunolocalization was observed in the secretory tip of the ameloblasts (X100 DIC). Note that the condensed STI and SR is an artifactual immunolocalization of laminin.

Note: AB = Ameloblasts; **OB** = odontoblasts; **PD** = predentin; **DP** = dental papilla; **BM** = basement membrane; **CV** = cervical loop; **STI** = stratum intermedium; **LAM** = laminin, **SR** = stellate reticulum

4.3 Gene expression

4.3.1 Amelogenin expression

The amelogenin gene was initially identified in a 6.5 day mouse pup first mandibular molar through the use of total mRNA extraction and DNA amplification by nested-PCR. The resultant ~200bp gene (Fig. 9) was then extracted and purified from a 1% agarose gel and sent for sequencing by Inqaba Biotech Laboratories. Since the ~200bp gene was detected in conjunction with primer dimer formation (Fig. 9) and other possible DNA contamination, it was necessary to do sequencing in order to confirm that this nucleotide fragment constituted part of the mouse amelogenin gene. A nucleotide-based search, BLASTn, (www.pubmed.com) illustrated that the extracted DNA band aligned perfectly with a section of the original amelogenin gene (Fig. 10) from which the primers were designed. The partial amelogenin mRNA transcript was found to be amplified and was expressed in all cultured molar explants that included 14.5 day (n=6) and 16.5 day (n=6) control explants as well as the samples treated with citral- (n=6 [14.5 day]; n=6 [16.5 day]) and wortmannin- (n=6 [14.5 day]; n=6 [16.5 day]).

4.3.2 Laminin α5 expression

The laminin α5 gene was originally identified in a 6.5 day mouse pup first mandibular molar by total mRNA extraction and amplification from the resultant cDNA with the use of nested-PCR. A ~215bp primer was designed from the known

nucleotide sequence of the mouse laminin α5 gene. The amplification of this DNA band via nested-PCR was observed on a 1% agarose gel (Fig. 11). Since the nucleotide fragment was detected at the correct size without the presence of primer dimers and any other contamination, no sequencing was necessary in this case. With the aid of this data, the laminin α5 partial primer sequence was found to be amplified and expressed in all 14.5 day (n=6) and 16.5 day (n=6) control murine molar explants, together with those treated for 5-hour s with citral (n=6 [14.5 day]; n=6 [16.5 day]) or wortmannin (n=6 [14.5 day]; n=6 [16.5 day]).

4.4. Quantitative Real-time Polymerase Chain Reaction

4.4.1 QRT-PCR Amelogenin

QRT-PCR analysis was performed to compare the difference in amelogenin gene expression between the 14.5 day and 16.5 day embryonic control first molar explants with those of the 14.5 day and 16.5 day citral- or wortmannin-treated first molar explants (Fig. 12).

The analysis revealed that there was no significant change ($P \leq 0.05$) in amelogenin expression between the 14.5 day and 16.5 day control molar explants (Fig. 12). When the amelogenin expression of the 14.5 day control molars and the 14.5 day citral-treated molars was compared, amelogenin gene expression of the 14.5 day citral-treated molars had significantly increased ($P>0.05$; Appendix C) with regard to that of the 14.5 day control and the 16.5 day citral-treated molar explants (Fig 12).

However statistical analysis revealed that the amelogenin expression in the 16.5 day citral-treated molar explants was not significantly different from that of the 16.5 day control molar explants ($P<0.05$). When the 16.5 day molar explants treated with wortmannin were compared to the 16.5 day control molars, amelogenin gene expression was also not significantly different ($P<0.05$; Appendix E). Furthermore, there was no significant difference ($P<0.05$) in amelogenin-mRNA synthesis between the 14.5 day wortmannin-treated molar explants and the 14.5 day control molar explants (Fig.12). When comparing the 14.5 day wortmannin-treated explants with the 16.5 day wortmannin-treated explants, no significant difference ($P<0.05$) in amelogenin-mRNA levels were detected.

4.4.2 QRT-PCR Laminin α5

QRT-PCR was performed in order to assess the expression of the laminin α5 gene in control explants of 14.5 day and 16.5 day explants cultured for 12 days, with their corresponding citral- or wortmannin-treated first molar explants. The difference in laminin α5 expression between the 14.5 day and 16.5 day control first molars was statistically insignificant (Appendix E) (Fig. 13).

The 14.5 day citral-treated embryonic mouse first molars showed no significant difference ($P>0.05$; Appendix E) in laminin α5 gene expression compared to the 14.5 day control first molars. The laminin α5 gene expression in the 16.5 day citral-treated

first molar explants was also not significantly different ($P<0.05$) when compared to the 16.5 day control first molar explants. When comparing 14.5 day citral-treated molars to their 16.5 day citral-treated counterparts, the statistics revealed that they were not significantly different ($P<0.05$). When 14.5 day wortmannin-treated first molars and 14.5 day control first molars were compared, again there was no significant difference ($P>0.05$) in laminin α5 expression to that of the control first molar explants (Fig. 13). A significant difference ($P>0.05$) in laminin α5 gene expression between the 16.5 day wortmannin-treated first molars and the 16.5 day control first molar explants was not detected. Neither was a significant difference found when the 16.5 day wortmannin-treated explants were compared with the 14.5 day wortmannin-treated first molars.

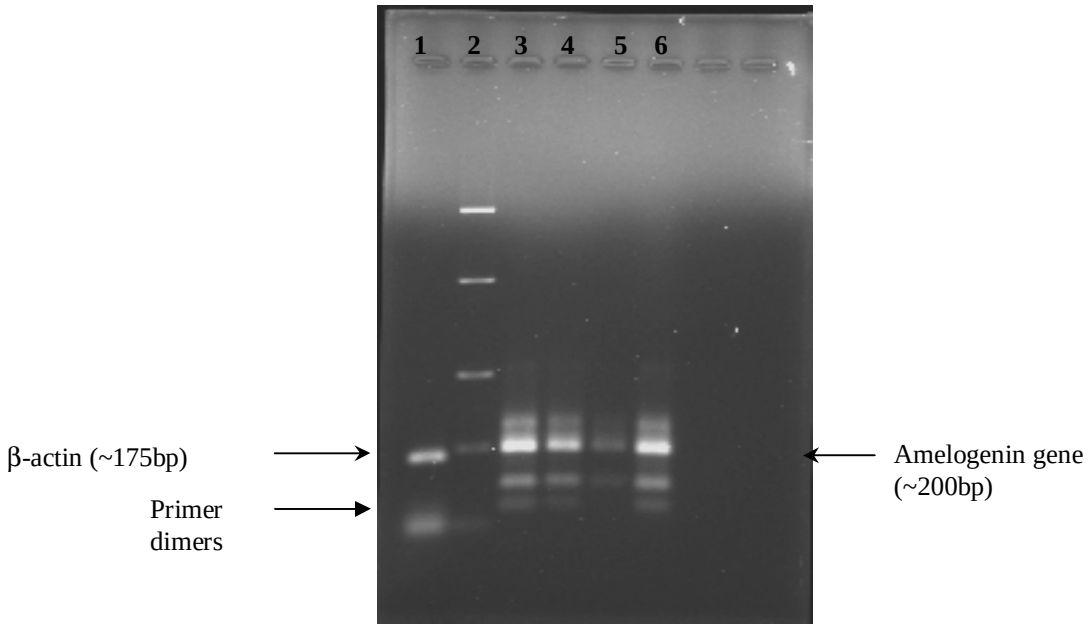

Figure 9. Amelogenin gene expression using nested-PCR.
Lane 1: β-actin housekeeping gene
Lane 2: DNA Ladder, Low Range
Lane 3-6: Different dilutions of cDNA starting product amplified for amelogenin

```
>ref|NM_009666.2| Mus musculus amelogenin X chromosome (Amelx), mRNA
Length=808

 Score =  123 bits (136),  Expect = 2e-26
 Identities = 103/116 (88%), Gaps = 9/116 (7%)
 Strand=Plus/Plus

Query  5    CAGAGCATGATAAG-CAGCCGTATCCTTC-TATG-TTACGAACCA--GGGTGAGAGGCTG  59
            ||||||||||||||| |||||||||||||| |||| |||||||||   |||||   |||||
Sbjct  195  CAGAGCATGATAAGGCAGCCGTATCCTTCCTATGGTTACGAACCCATGGGTGGATGGCTG  254

Query  60   CACCACCAAATC-TCCCTG-GCTGTCTCAACAGC-TCCCCCGAG-CACACCCTTCA  111
            |||||||||||| |||||| |||||||||||||| ||||||||| ||||||||||
Sbjct  255  CACCACCAAATCATCCCTGTGCTGTCTCAACAGCATCCCCCGAGTCACACCCTTCA  310
```

Figure 10. BLASTn sequence alignment analysis indicating that the extracted DNA band is the amelogenin sequence initially selected to be amplified by the primers. **Note:** The sequence is slightly shorter than expected which is caused by the loss of nucleotides during the sequencing process.

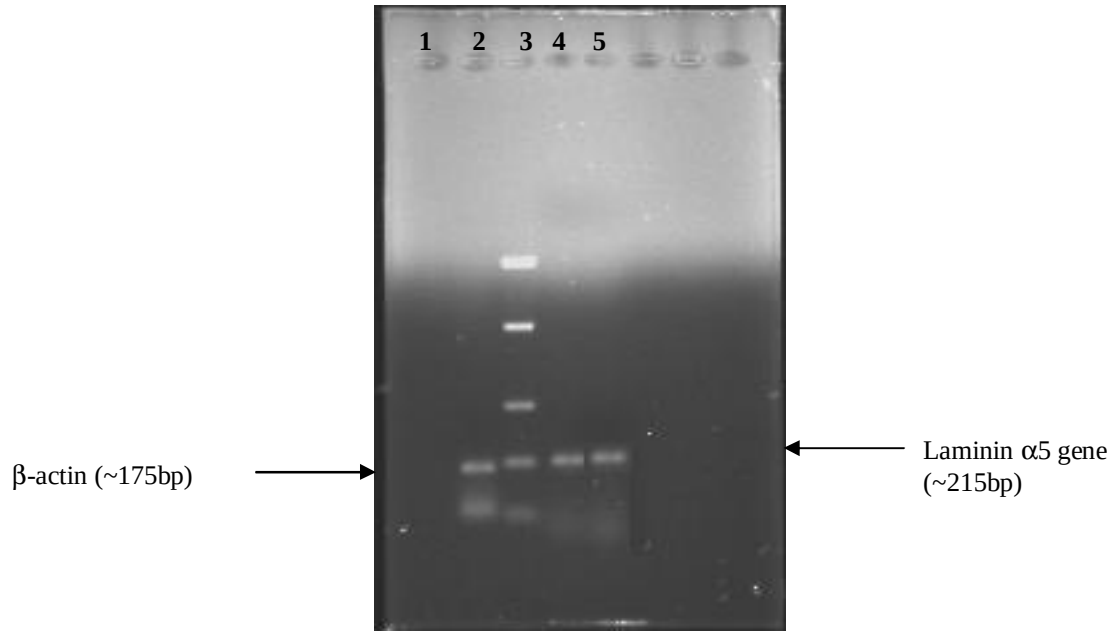

Figure 11. Laminin α5 gene expression using nested-PCR.
Lane 2: β-actin housekeeping gene
Lane 3: DNA Ladder, Low Range
Lane 4-5: cDNA from 6.5 day neonatal mouse pup first mandibular molars amplified for laminin α5.

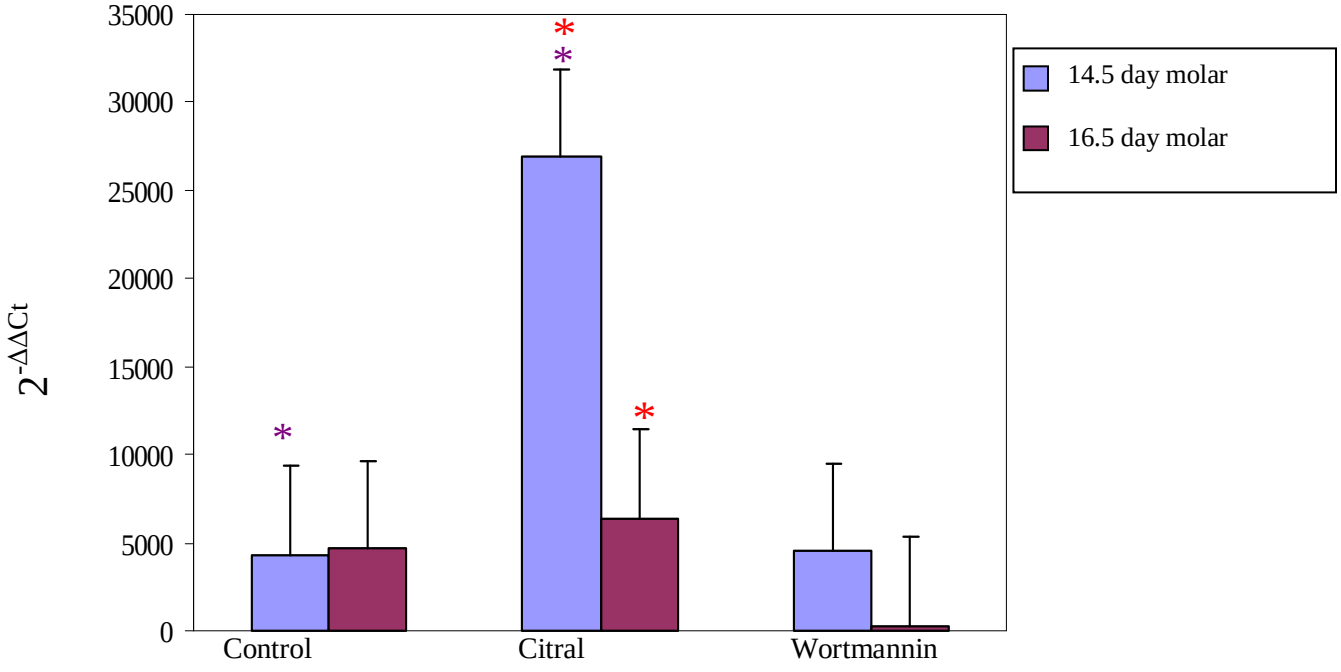

Figure 12. Graphical representation of the relative amelogenin gene expression of 14.5 day and 16.5 day first mandibular molars. Explants were cultured as controls or treated with citral for 5-hour s or were exposed to wortmannin for 5-hour s.
*, * = Significantly different **Note:** The same coloured stars on top of two groups e.g. control and citral denotes that they are significantly different from each other.

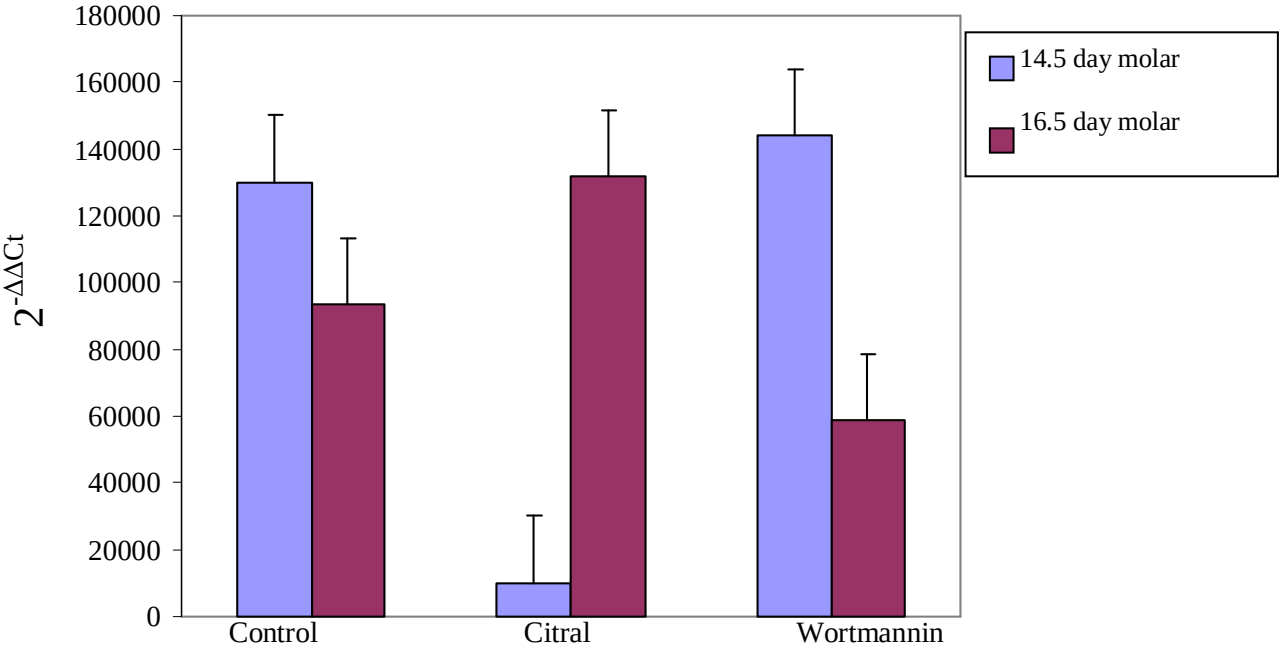

Figure 13. Graphical representation of the relative laminin gene expression of 14.5 day and 16.5 day embryonic first mandibular molars. Explants were either grown as controls, treated with citral or were exposed to wortmannin.
Note: None are significantly different

5. Discussion

5.1 Approaches to regulating enamel thickness and enamel patterning (cusp morphology)

The current work explored the different ways in which enamel thickness and cusp morphology of the first mandibular molars of embryonic mice could be regulated or perturbed, as this may bear on the adaptation of teeth during the course of evolution. Two reactions bear on enamel and cusp formation, namely amelogenin in relation to enamel formation, and laminin which regulates differentiation of ameloblasts and odontoblasts. To perturb these reactions two inhibitors were used namely citral, which inhibits RA synthesis, and wortmannin, which prevents PI3K activation resulting in inhibition of laminin production. These steps are depicted in figure 14.

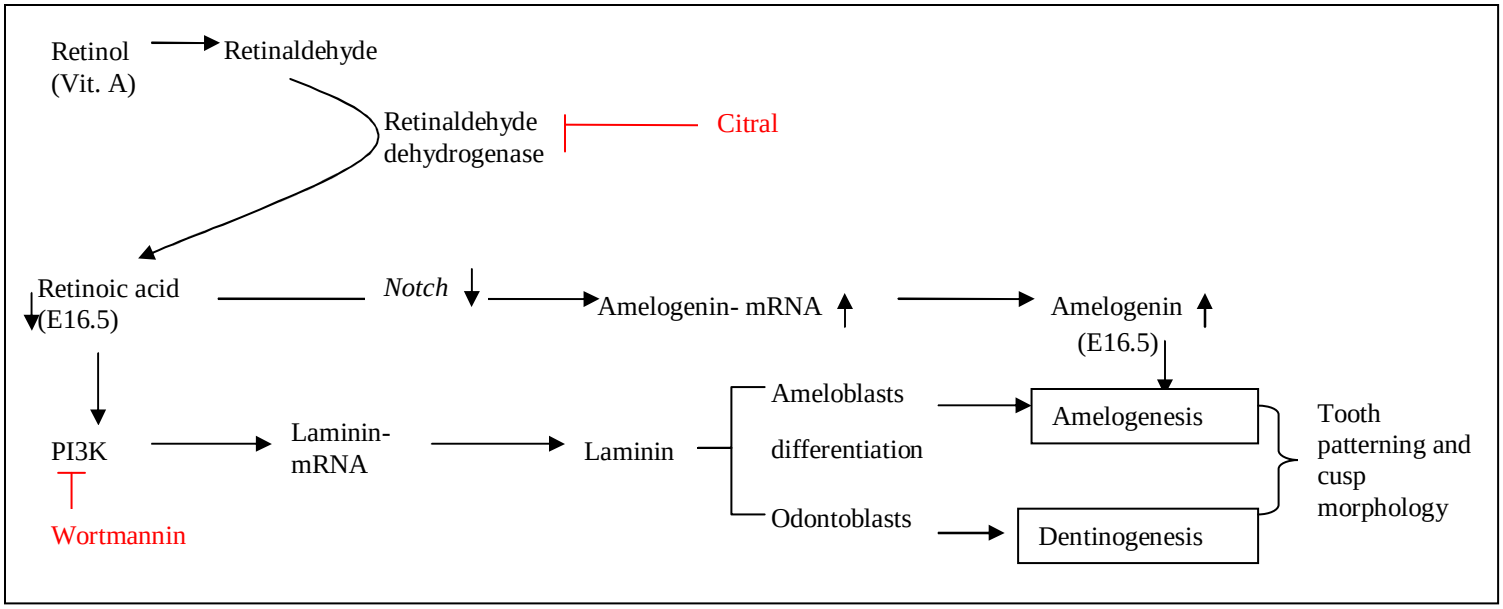

Figure 14. Reaction sequence depicting the effect of retinoic acid (RA) on gene expression of amelogenin and laminin. In normal development RA is lowered on embryonic day 16.5 (Niederreither *et al.*, 2002) which is correlated with the downregulation of Notch and an increase in amelogenin-mRNA. Citral can inhibit retinaldehyde dehydrogenase, which should lead to decreased RA concentrations before embryonic day 16.5 (Kronmiller *et al.*, 1995a). Subsequently RA regulates PI3K activation by PDGF (Pedigo *et al.*, 2007) which modulates laminin gene expression. Laminin controls the differentiation of ameloblasts and odontoblasts which in turn regulate tooth patterning and cusp morphology (Eltit and Oyarzin, 2007)

Couwenhoven and Snead (1994) showed that whereas RA is high at the bud stage and low after the bell stage of tooth development, amelogenin is low at the bud to cap stage but higher after the bell stage (Fig. 15). Would a premature lowering of the level of RA lead to a premature burst of amelogenin synthesis, as reflected in terms of amelogenin mRNA levels and a changed morphology?

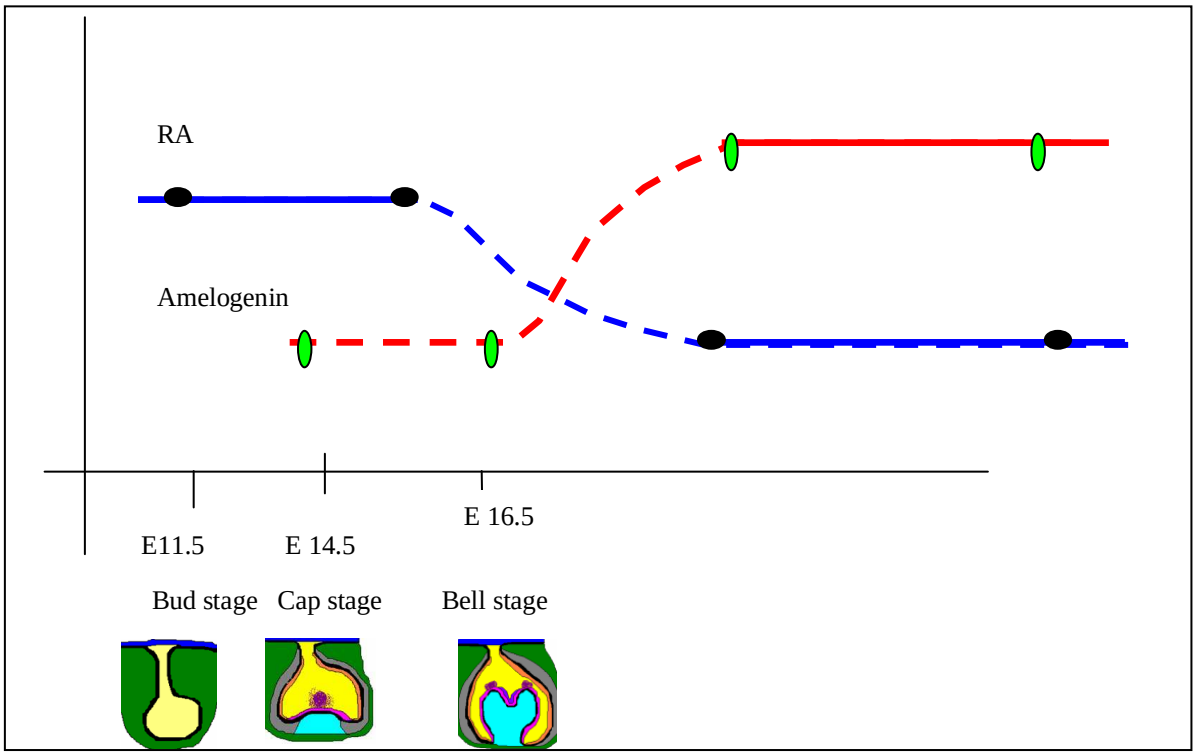

Figure 15. Diagrammatic representation which shows that, under normal growth conditions, when retinoic acid (RA) decreases at embryonic day 16.5 amelogenin levels increase (Couwenhoven and Snead, 1994; Niederreither *et al.*, 2002).

Niederreither *et al.*, 2002 Couwenhoven and Snead, 1994

In the first part of the discussion the effect of citral and wortmannin treatments on the morphology and histology of embryonic first mandibular molars in mice will be addressed. In the second part the level of mRNA which promotes amelogenin-mRNA and laminin-mRNA synthesis will be addressed.

5.1.1 *In vitro* development of embryonic mouse molars and the effects of citral and wortmannin on the morphology, histology and protein synthesis

The results from the present study revealed that teeth cultured *in vitro* for 12 days did not develop to the late bell stage of tooth development. Treated and controls control molar explants from the 14.5 and 16.5 day groups had only reached the mid-bell stage, when compared to the normal *in vivo* development of the first mandibular molar from a 6.5 day mouse pup. Morphologically, the teeth appeared to be smaller than the *in vivo* first molar but possessed a normal multicusped shape. However the formation of enamel was absent in the cultured teeth, even though immunocytochemically amelogenin synthesis was detected in the 14.5 and 16.5 day control and citral-and wortmannin-treated molar explants. Immunocytochemistry for laminin in the 14.5 and 16.5 control or citral-treated first molar explants was detected in ameloblasts and odontoblasts including at the junction of the ameloblast and predentin layer, which suggests that the basement membrane was still in the process of being degraded. This led to the hypothesis that all cultured teeth, upon extraction from their *in vivo* environment experienced a very slow rate of development, which resulted in the cultured first mandibular molars reaching the mid-bell stage of tooth development, which is characterized by ameloblast/odontoblast differentiation, the start of amelogenesis, the presence of an intact basement membrane and the presence of a pre-dentin layer but no enamel matrix.

Hay (1961) in her research on the development of *in vitro* and *in vivo* mouse incisors and molars showed that molars of mice cultured *in vitro* experienced a very slow rate of development. Under normal *in vivo* conditions teeth cultured from either the cap stage (E14.5) or early bell stage (E16.5) for 12 days reached approximately the 6^{th} day of post-

natal development. Histologically, the cells of the various tissue layers of the molar, such as the inner enamel epithelium and the outer enamel epithelium would have differentiated by embryonic day 16 to 17 into their specific cell types i.e. ameloblasts and odontoblasts respectively, with nuclei migrating away from these cells' apical pole. The stratum intermedium would have formed deep to the ameloblasts to assist with controlling enamel production (Cohn, 1957; Hay, 1961). Thick extracellular matrices such as predentin, dentin and enamel would have been formed by postnatal day 6 (Hay, 1961), as was seen in the 6.5 day pup in the present study. The process of amelogenesis would have reached the mature stage of development, i.e. amelogenin content of enamel is being replaced by hydroxyappatite crystals and calcium/phosphate ions (Hay, 1961). The results of Hay (1961) indicated that the developing mouse teeth when cultured *in vitro*, irrespective at what stage of tooth development they were extracted at, developed only for a certain period, i.e. cap stage to bell stage, before they ceased all development. Hay (1961) suggests that it is a matter of culture technique utilized and that during extraction the tooth can become damaged, which may affect the rate of tooth development. On the other hand, Black (1999) suggests that the variation in diffusion distance of cells in a tissue *in vitro*, could lead to decreased developmental rates of cells or tissues located near the centre of the organ. If the central cells of the developing embryonic molar, such as ameloblasts, odontoblasts and those cells of the stellate reticulum/stratum intermedium, did not receive adequate nutrients to replicate, then it could explain why there was a slowing down in development. However, Black's (1999) suggestion may not be related to the current experiment, because if this had been the case, then ameloblasts would not have been able to produce amelogenin. Therefore it is suggested that it is most likely due

to the extraction procedure and the time taken to transfer the explants into an environment, which caused molar explants to develop slowly in the current experiment.

When interpreting the results of the effects of citral and wortmannin on the development of the first molar. results showed that these treatments did not affect the histology, morphology or protein synthesis of these explants. Laminin was detected in both the ameloblast and odontoblast cell layers, in both 14.5 and 16.5 day molar explants (control and treated), indicating that neither citral nor wortmannin had an inhibitory effect. Fukumoto *et al.* (2005) found that cusps of molars were "welded" together or that the tips of the cusps were flat following wortmannin treatment. However following wortmannin treatment in the present study the cusps were spaced out normally and were pointy. These results therefore suggest that the exposure period of 5 hours compared to the 24 hours used by Fukumoto *et al.* (2005) was possibly inadequate to affect cusp morphology and the synthesis of proteins such as laminin and amelogenin. Both Kronmiller *et al.* (1995a) and Fukumoto *et* al. (2005) in their tissue culture experiments on tooth development treated the teeth at the bud stage and/or cap stage with either citral or wortmannin respectively, for 24 hours, to produce changes in tooth development and the shape of the cusps. It is therefore feasible to repeat the current experiment utilizing different exposure periods set above the 5 hour mark and see whether this causes any changes in cusp morphology

5.1.2 The effect of citral and wortmannin on amelogenin-mRNA synthesis during molar development

The results of the current experiment show that there is an early onset of amelogenin-mRNA synthesis following citral treatment. This early onset of amelogenin-mRNA occurs in embryos treated at stage 14.5 which is well before the normal onset of amelogenesis at day 16.5 of tooth development (Zeichner-David *et al.,* 1995). However, in embryonic mouse molars treated at day 16.5, a stimulatory effect of citral on the level of amelogenin-mRNA was not observed. The interpretation of this finding is in accordance with published data by Mitsiadis *et al*. (1995), Coffman *et al.* (1993) and Kronmiller *et al*. (1995a) who suggested that a lowering of the RA concentration correlates with the initiation of amelogenesis during tooth development. The pathway involved in amelogenin synthesis is depicted in figure 14 where it is seen that the conversion of retinol to retinoic acid may be inhibited by citral, thereby causing a pre-amelogenin-mRNA synthesis, i.e. before day 16.5 the time of normal amelogenesis (Fig. 15). This early onset of increased amelogenin-mRNA levels may be interpreted in terms of two possible feedback circuits that could control the levels of amelogenin-mRNA (Fig. 16). In this regard it is suggested that while citral treatment at day 14.5 of development causes a pulse in amelogenin-mRNA in day 14.5 treated explants, there is a lag before amelogenin-protein accumulates to its normal level (at day 16.5).

In the normal situation, it is suggested that the level of amelogenin-mRNA is regulated by the equilibrium between its synthesis and breakdown. In day 16.5 treated embryonic molars, synthesis and breakdown are in equilibrium. However, it is here suggested that while in 14.5 day embryonic molars treated with citral there is an early onset of

amelogenin-mRNA, the degradative mechanisms that regulate its level are not yet operative.

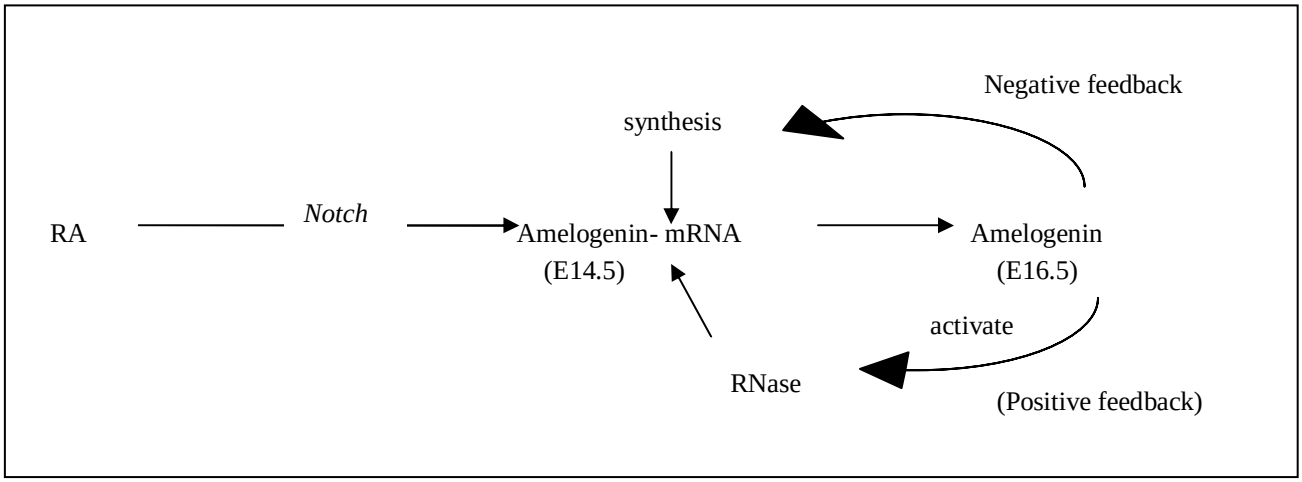

Figure 16. Two feedback systems that could control the level of amelogenin-mRNA. The first is amelogenin protein feeding back negatively to inhibit mRNA production where the second causes the activation of RNase to degrade excess mRNA levels.

One can postulate two types of mechanisms that maintain the level of mRNA over and above the particular molecular structure of amelogenin-mRNA which may also contribute to the stability. Firstly the negative feedback effect of amelogenin on its synthesis, and secondly the activation effect of amelogenin on promoting RNase activity (Fig. 16). Thus in the presence of too much amelogenin, the latter could act as a feedback inhibitor whereby it binds to elements in the synthesis pathway. However it could also be possible that too much amelogenin-mRNA could feedback and activate RNase. The regulation of mRNA levels is dependant on the structure of mRNA in terms of the G-C (guanine-cytosine) content (Ativater *et al.*, 1990) and the presence or absence of long poly (A) tails at the 3'-end (Valencia-Sanchez *et al.*, 2006). Factors such as RNA interference molecules (RNAi) may also have an effect on mRNA levels, but nothing is known about

this at present. Thus, if amelogenin mRNA is synthesized ahead of the stage at which the mechanisms that control its concentration are operational, its concentration may go unchecked and tend to overshoot its appropriate level. That the level of amelogenin-mRNA may be under strict control opens up the possibility of modulating amelogenin-mRNA in normal tooth development and consequently in enamel thickness all of which bears on the regulatory mechanisms upon which natural secretion may act in the shaping of tooth morphology.

In terms of the wortmannin inhibition of PI3K, results from the current work showed that the amelogenin-mRNA levels were not affected when PI3K activation was inhibited by wortmannin. The PI3K pathway (Fig.17) is primarily involved in regulating laminin-mRNA via protein kinase B/Akt (Li *et al.*, 2001). There is no indication in the literature that PI3K regulates amelogenin. Since no changes in cusp formation were observed in the present study and there was no change in amelogenin-mRNA levels it can be suggested that the exposure period of 5 hours to wortmannin was not long enough to induce any effective change in either morphology or at a genetic level. However, because a sample size of 6 molars was used to compile the data, it cannot be excluded that the number of molars used in the current experiment was too small and thus no significant difference could be detected when analyzed. On the other hand changes in cusp morphology do not appear to be related to events involved in the amelogenin-mRNA synthesis pathway, even though wortmannin is presumed to affect enamel patterning and cusp morphology. Therefore, it may be profitable to revisit these finding using a larger sample size and to see whether longer exposure periods yield different results.

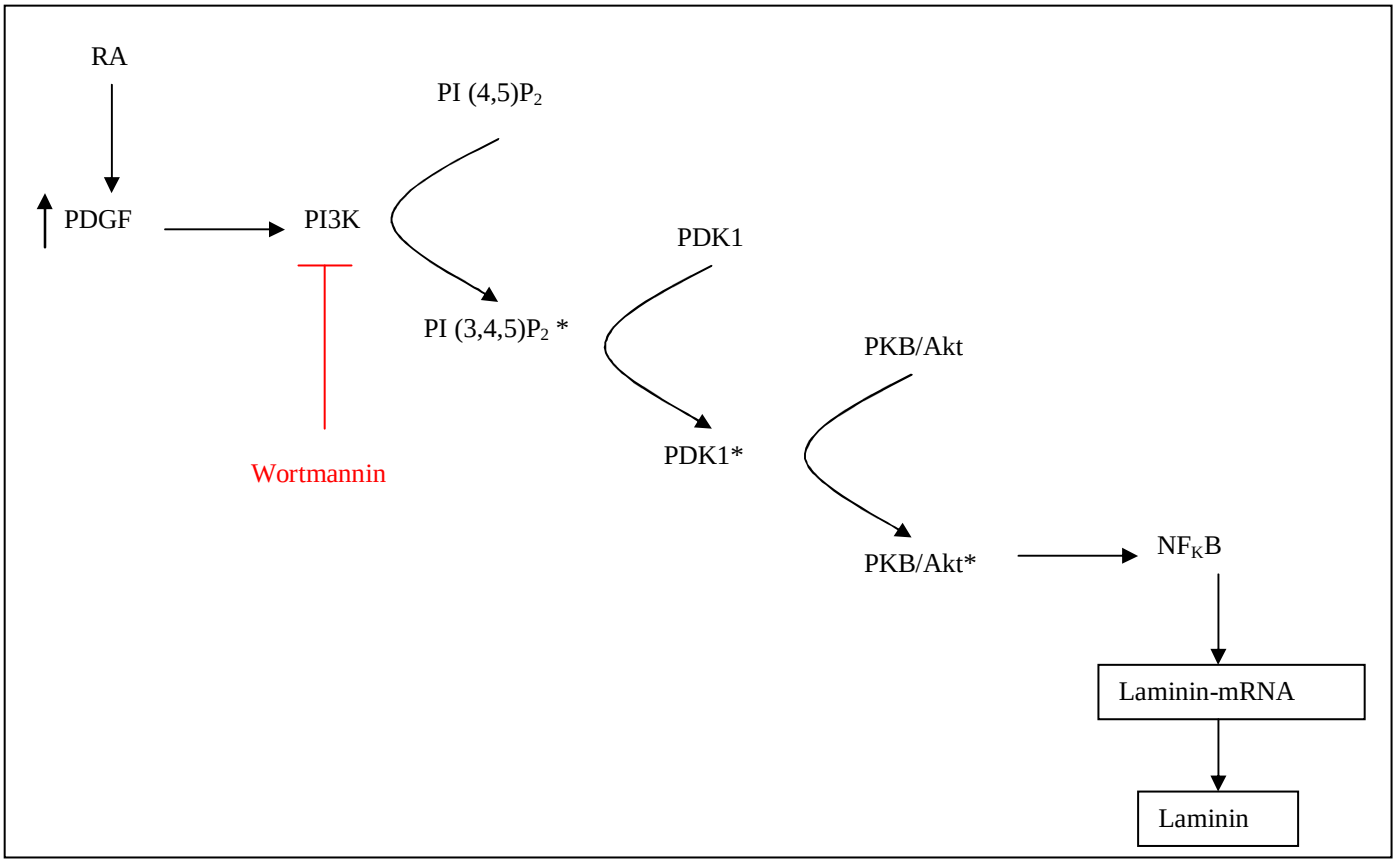

Figure 17. Reaction sequence depicting the control of laminin gene expression by phosphoinositol-3-kinase (PI3K). Under normal conditions platelet derived growth factor (PDGF) is upregulated by retinoic acid (RA) (Pedigo *et al.*, 2007), which binds with receptors that have the inactive PI3K component. Once released from the receptor PI3K phosphorylates PI (4, 5)P_2 to its active form PI (3,4,5)P_2 (Cantley, 2002). The PI (3,4,5)P_2 then activates protein dependant kinase 1 (PDK1) by phosphorylation which in turn phosphorylates protein kinase B (PKB)/Akt (Cantley, 2002). The Akt activates the NF_KB pathway which then upregulates laminin-mRNA production (Li *et al.*, 2001). Wortmannin inhibits PI3K activation and subsequently laminin gene expression.

5.1.3 The effect of wortmannin and citral on the levels of laminin α5-mRNA

The findings of the present study did not show any variation in laminin α5-mRNA synthesis when either PI3K or RA were inhibited with wortmannin or citral respectively. Although it was thought that a loss in either PI3K or RA could have an effect on laminin-mRNA synthesis (Fig. 17) in molar explants treated with citral at day 14.5 of development, a statistical analysis of the results showed that citral had no significant effect on laminin-mRNA synthesis. Laminins are a diverse group of proteins which are secreted from cells to form specialized cellular derivatives, such as the basement membrane which helps to regulate cellular processes. This has been especially shown in tooth development in which the laminins, especially laminin α5 in the basement membrane, are suggested to regulate the differentiation of ameloblasts of the inner enamel epithelium and odontoblasts of the dental papilla (Eltit and Oyarzin, 2007). It is therefore strange that wortmannin and citral, which inhibit PI3K activation and RA synthesis respectively, did not cause a change in laminin-mRNA levels. This suggests one of four possibilities: (1) These inhibitors did not effectively target the PI3K and RA sites in these experiments. (2) The sample size of six molars treated with either citral or wortmannin on which qRT-PCR was performed was inadequate to show a change in gene expression when citral or wortmannin were applied to first mandibular molar explants. (3) Variation in qRT-PCR C_t values, could suggest that laminin-mRNA was a direct result from different rates of synthesis in the embryonic molars or from the well known instability of mRNA during its extraction. (4) There are possibly other pathways which operate parallel to the PI3K pathway, or by cross-talk, which function to maintain the appropriate level of laminin α5-mRNA. It would therefore be appropriate in future

experiments to monitor the level of Akt and other PI3K pathway proteins to see how these other PI3K pathway proteins alter their activity status when PI3K or RA syntheses are altered.

6. Conclusion

Citral and wortmannin had no effect on the morphology, histology and immunolocalization of amelogenin or laminin of 14.5 day and 16.5 day first mandibular molars, in an *in vitro* system. However, the current study did provide evidence that a loss in RA, via citral inhibition, before the onset of amelogenesis at day 16.5 can lead to an early increase in amelogenin-mRNA levels. Once amelogenesis occurs and RA decreases, feedback and degradative mRNA systems become operational, which possibly regulate the synthesis of amelogenin-mRNA levels. PI3K does not seem to be involved in regulating amelogenin expression. As for laminin α5-mRNA, the study is uncertain on whether PI3K or RA may be involved in regulating this gene's expression.

7. References

1. Apajalahti, S. 2004. Short root anomaly (SRA). Institute of Dentistry, University of Helsinki, Finland 1:1-79 (http://ethesis.helsinki.fi/julkaisut/laa/hamma/vk/apajalahi/)

2. Ativater, A.J., Wisdom, R., and Verma, I.M. 1990. Regulated mRNA stability. Annu Rev Genet 24: 519-541

3. Avery, J.K. 2001. Oral development and histology 3rd ed. Thieme Medical Publishers, New York, U.S.A. Chapter 9-12

4. Berkovitz, B.K.B., Maden, M., McCaffery, P. and Barrett, A.W. 2001. The distribution of retinaldehyde dehydrogenase-2 in rat and human orodental tissues. Arch Oral Biol 46: 1099-1104

5. Black, J. 1999. Biological performance of materials-fundamentals of biocompatibility 4th ed. Marcel Dekker, Inc., New York. 17-21

6. Cantley, L.C. 2002. The phosphoinositide 3 kinase pathway. Sci 296: 1655-1657

7. Cobourne, M.T. 1999. The Genetic control of early odontogenesis. British J Orthod 26: 21-28

8. Cobourne, M.T. and Sharpe, P.T. 2003. Tooth and jaw: molecular mechanisms of patterning in the first branchial arch. Arch Oral Biol 48: 1-14

9. Coffman, C.R., Skoglund, P., Harris, W.A. and Kintner, C.R. 1993. Expression of an extracellular deletion of Notch diverts cell fate in *Xenopus* embryos. Cell 73: 671-695

10. Cohn, S. 1957. Development of the molar teeth in the albino mouse. Americ J Anat 101: 295-318

11. Couwenhoven, R.I., and Snead, M.L. 1994. Early determination and permissive expression of amelogenin transcription during mouse mandibular first molar development. Dev Bio 164: 290-299

12. Eltit, F., and Oyarzin, A. 2007. Immunolocalization of integrin 4 during the amelogenesis. Eu Cells and Materials 14: 1473-2262

13. Fukumoto, S., Kiba, T., Iehara, B., Nakamura, T., Longenecker, G., Krebsbach, P.H., Kulkarni, A.B. and Yamada, Y. 2004. Ameloblastin is a cell adhesion molecule required for maintaining the differentiation state of ameloblasts. J Cell Biol 167: 973-983

14. Fukumoto, S., Miner, J.H., Ida, H., Fukumoto, E., Yuasa, K., Miyazaki, H., Hoffman, M.P. and Yamada, Y. 2005. Laminin α5 is required for dental epithelium growth and polarity and the development of tooth bud and shape. J Biol Chem 8: 5008-5016

15. Gilbert, S.F. 1994. Developmental Biology 4th ed. Sinauer Associates Inc., Massachusetts, U.S.A.

16. Hay, M.F. 1961. The development *in vivo* and *in vitro* of the lower incisor and molars of the mouse. Arch Oral Biol 3: 86-109

17. Huq, M.D.M., Tsai, N.-P., Khan, A., and Wei, L.-N. 2007. Lysine trimethylation of retinoic acid receptor-α (RARα): A novel means to regulate receptor function. Mol Cell Proteom 1-38

18. Iwasaki, K., Bajenova, E., Somogyi-Ganss, E., Miller, M., Nguyen, V., Nourkeyhani, H., Gao, Y., Wendel, M. and Ganss, B. 2005. Amelotin a novel secreted ameloblasts-specific protein. J Dent Res 12: 1127-1132

19. Kronmiller, J.E., Beeman, C.S., Nguyen, T. and Berndt, W. 1995(a). Blockade of the initiation of murine odontogenesis *in vitro* by citral, an inhibitor of endogenous retinoic acid synthesis. Archs oral Biol 40: 645-652

20. Kronmiller, J.E., Nguyen, T. and Berndt, W. 1995(b). Instruction by retinoic acid of incisor morphology in the mouse embryonic mandible. Archs Oral Biol 40: 589-595

21. Koyama, E., Wu, C., Shimo, T., Iwamoto, M., Ohmori, T., Kurisu, K., Ookura, T., Bashir, M.M., Abrams, W. R., Tucker, T. and Pacifici, M. 2001. Development of

stratum intermedium and its role as a *Sonic hedgehog*-signalling structure during odontogenesis. Dev Dynam 222: 178-191

22. Li, X., Talts, U., Talts, J.F., Arman, E., Ekblom, P. and Lonai, P. 2001. Akt/PKB regulates laminin and collagen IV isotypes of the basement membrane. PNAS 98: 14416-14421

23. Miletich, I., and Sharpe, P.T. 2003. Normal and abnormal dental development. Human Mol Gen 12: 69-73

24. Mitsiadis, T.A., Lardelli, M., Lendahl, U. and Thesleff, I. 1995. Expression of Notch 1, 2, and 3 is regulated by epithelial-mesenchymal interactions and retinoic acid in developing mouse tooth and associated with determination of ameloblasts cell fate. J Cell Biol 130: 407-418

25. Moss-Salentijn, L., and Hendricks-Klyvert, M. 1990. Dental and oral tissues 3rd ed. Lea and Febiger, Pennsylvania, U.S.A. 147-157

26. Niederreither, K., Fraulob, V., Garnier, J., Chambon, P., and Dolle, P. 2002. Differential expression of retinoic acid-synthesizing (RALDH) enzymes during fetal development and organ differentiation in the mouse. Mech Dev 110: 165-171

27. Pedigo, N.G., Zhang, H., Mishra, A., McCorkle, J.R., Ormerod, A.K. and Kätzel, D.M. 2007. Retinoic acid inducibility of the human PDGF-a gene is mediated by distal DNA motifs that overlap with basal enhancer and vitamin D response elements. Gene Expr 14: 1-12

28. Sanes, J.R. 2003. The basement membrane/basal lamina of skeletal muscle. J Biol Chem 15: 12601-12604

29. Schuh, T., Hall, B., Creech Kraft, J., Privalsky, M. and Kimmelman, D. 1993. V-erb and citral reduce tertagenic effects of all-*trans*-retinoic acid and retinol, respectively, in *Xenopus* embryogenesis. Dev 119: 785-798

30. Stephanopoulos, G., Garefalaki, M.-E., and Lyroudia, K. 2005. Genes and related proteins involved in amelogenesis imperfecta. J Dent Res 84: 1117-1126

31. Teaford, M.F., Smith, M.M., and Ferguson, M.W.J. 2000. Development, function and evolution of teeth. Cambridge University Press, UK. 1.2: 4-5

32. Torres-Quintana, M.A., Gaete, M., Hernandez, M., Farias, M., and Lobos, N. 2005. Ameloblastin and amelogenin expression in postnatal developing mouse molars. J Oral Sci 47: 27-34

33. Valencia-Sanchez, M.A, Liu, J., Hannon, G.J., and Parker, R. 2006. Control of translation and mRNA degradation by miRNAs and siRNAs. Gen Dev 20: 515-24

34. Yurchenco, P.D., Amenta, P.S. and Patton, B.L. 2004. Basement membrane assembly, stability and activities observed through a developmental lens. Matrix Bio 22: 521-538

35. Zeichner-David, M., Diekwisch, T., Fincham, A., Lau, E., MacDougall, M., Moradian-Oldak, J., Simmer, J., Snead, M., and Slavkui, H.C. 1995. Control of ameloblast differentiation. Int J Dev Biol 39: 69-92

8. Appendices

Appendix A

1. Solutions for tissue extraction

Calcium and magnesium-free Tyrode's solution (1000ml) made up of three solutions

Solution 1

500ml dH_2O

2.0g NaCl

0.05g KCl

0.012g $NaH_2PO_4H_2O$

Solution 2

480ml dH_2O

0.025g $NaHCO_3$

Solution 3

20ml dH_2O

1g $C_6H_{12}O_6$

Saline solution

1M NaCl

2. Solutions for tissue fixation and staining

Formic citric acid (decalcification solution)

1% CH_2O_2

10% $Na_3C_6H_5O_7.2H_2O$

Adjusted to pH 5 with 5M HCL

10% buffered formalin (fixative)

4% HCHO

3.5g $NaH_2PO_4.H_2O$

6.5g Na_2HPO_4

Hematoxylin

2g $C_{16}H_{14}O_6$

0.2g $INaO_3$

17.6g $Al_2O_{12}S_3$

250g $C_2H_6O_2$

730ml dH_2O

Filter before use

Eosin

2.5g Sodium Tetrabromofluorscein

500ml dH_2O

5M HCL

Dissolve the Eosin (Sodium Tetrabromofluorscein) in the water and slowly add the hydrochloric acid which combines with the sodium. The resulting precipitate is the acid form of tetrabromofluoroscein which is insoluble in water. Allow the precipitate to settle, and decant the supernatant fluid. Add about 500 ml of distilled water to the precipitate and stir until the dye is well suspended, then allow to settle. Repeat the washing process about six times to remove all the traces of sodium and chloride ions. Filter and allow the filter paper and dye to dry in a drying oven (60°). Remove the dye from the paper and pulverize it in a mortar. Weigh the pulverized dye and dissolve it in the proportion of 100 ml of 95% alcohol for each 0.5 g of dye

3. Solutions for Immunocytochemistry

PBS

0.58g NaCl

1.42g Na_2HPO_4

1.20g $Na_2H_2PO_4.2H_2O$

950ml dH_2O

Adjust to pH 7.1

EDTA (antigen retrieval)

0.37g $C_{10}H_{16}N_2O_8$

1000ml dH_2O

Adjust to pH 8.0

Tris-saline

0.95% NaCl

0.05M Tris/HCl (pH 7.6)

Diluent for antisera

100ml Tris-saline

0.005g bovine serum albumin

0.04g $C_{10}H_{16}N_2O_8$

1ml swine serum

D.A.B. (3-3 Diaminobenzideinetetrahydrochloride)

2ml Tris/HCl (pH 7.6)

1% H_2O_2

Filter before use.

4. Storage buffers for primers

TE

10mM Tris/HCl (pH 8.0)

10mM EDTA (pH 8.0)

5. Buffers and solutions for Agarose Gel Electrophoresis

5X TBE

0.89M Tris

0.089M Boric Acid

0.002M EDTA

Adjust to pH 7.6

Agarose gels

2g (1%) or 2.8g (1.4%) Agarose

180ml dH_2O

20ml 5X TBE (pH 7.6)

Running Buffer

180ml dH_2O

20ml 5X TBE (pH 7.6)

Loading Buffer (Tracking dye)

30% Glycerol in TE

0.025% Bromophenol blue

10X Loading dye

0.25% Bromophenol blue

0.25% Xylene cyanol

50% Glycerol

0.25mM EDTA

6. Miscellaneous Stock

Antibiotic Stock

Streptomycin/ Penicillin 100mg/ml dissolved in dH_2O

Appendix B

DNA molecular weight markers used in this work

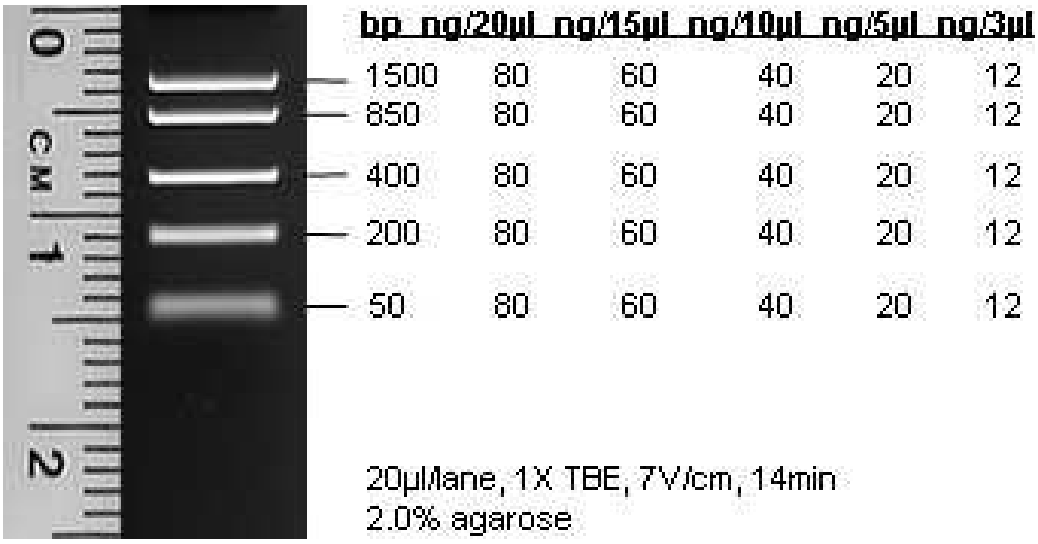

Figure 1B. FastRuler DNA Ladder. **Note:** Range **(**in bp): 1500, 850, 400, 200, 50.

Appendix C

Statistical formula

Paired t-test (Allan, 1982)

$t = m_x - m_y / SED_{mx-my}$ and $m_x - m_y$ = positive value

Where m_x = mean of first sample group

m_y = mean of second sample group

SED_{mx-my} = standard error between means

And t has $(n_x + n_y - 2)$ degrees of freedom

Where n = total number of samples compared to each other from each group

$SED_{mx-my} = \sqrt{[((sd_x)^2/n_x) + ((sd_y)^2/n_y)]}$

Where sd = standard deviation of sample

$sd_x = \sqrt{[(\sum x^2 - (\sum x)^2/n)/n-1]}$

Where n = total number of samples compared

Appendix D

Raw data of QRT-PCR run

1. $2^{-\Delta\Delta Ct}$ values for amelogenin expression

Type of tooth treatment, age and gene expression analyzed	$2^{-\Delta\Delta Ct}$ after QRT-PCR
Control 1 14.5 amelogenin	921.60
C2	59.76
C3	21424.89
C4	62.90
C5	222.40
C6	3326.98
	Mean = 4336.42
Control 1 16.5 amelogenin	114.80
C2	8761.73
C3	29.91
C4	56.77
C5	6080.61
C6	12819.03
	Mean = 4643.81
Citral 1 14.5 amelogenin	33970.62
Ci2	45292.98
Ci3	576.43
Ci4	14.75
Ci5	33947.10
Ci6	47544.80
	Mean = 26891.10
Citral 1 16.5 amelogenin	880.40
Ci2	23170.50
Ci3	10535.71
Ci4	4.94
Ci5	697.47
Ci6	2626.63
	Mean = 6400.76

Wortmannin 1 14.5 amelogenin	9809.75
W2	147.34
W3	16169.64
W4	917.14
W5	5.30
W6	20.99
	Mean = 4511.70
Wortmannin 1 16.5 amelogenin	199.33
W2	177.05
W3	946.86
W4	82.48
W5	56.45
W6	519.87
	Mean = 320.93

2. $2^{-\Delta\Delta Ct}$ values for laminin α5 expression

Type of tooth treatment, age and gene expression analyzed	$2^{-\Delta\Delta Ct}$ after QRT-PCR
Control 1 14.5 laminin α5	188.97
C2	772941.66
C3	117.30
C4	1666.96
C5	138.43
C6	7281.40
	Mean = 130139.12
Control 1 16.5 laminin α5	0.89
C2	87864.94
C3	3499.66
C4	43.23
C5	3970.21
C6	464719.29
	Mean = 93349.70

Citral 1 14.5 laminin α5	23854.93
Ci2	10.26
Ci3	193.47
Ci4	3.71
Ci5	29634.70
Ci6	6347.62
	Mean = 10007.45
Citral 1 16.5 laminin α5	9809.75
Ci2	620469.20
Ci3	376.90
Ci4	92361.25
Ci5	424.02
Ci6	65536.0
	Mean = 131496.19
Wortmannin 1 14.5 laminin α5	43.77
W2	205674.01
W3	721.10
W4	656301.86
W5	1.61
W6	221.78
	Mean = 143827.36
Wortmannin 1 16.5 laminin α5	277860.26
W2	46405.24
W3	232.50
W4	12.27
W5	28036.14
W6	142.62
	Mean = 58781.51

Appendix E

Raw data and statistical calculations of the QRT-PCR runs

1. t-test analysis (amelogenin expression)

Six samples were used for each group (e.g. Control 1 14.5 -Control 6 14.5).

:. $n_x = 6$ and $n_y = 6$

:. Degrees of freedom = $(n_x + n_y - 2) = 6 + 6 - 2 = 10$

:. t (P=0.05) = 2.23

:. Any calculated t values from two groups > 2.23 is deemed as significantly different

a.) Control 14.5 and Control 16.5

Control 14.5 (x)	**Control 16.5 (y)**	$(x)^2$	$(y)^2$
921.60	114.80	849346.56	13179.04
59.76	8761.73	3571.26	76767912.59
21424.89	29.91	459025911.5	894.61
62.90	56.77	3956.41	3222.83
222.40	6080.61	49461.76	3697381.97
3326.98	12819.03	11068795.92	164327530.1
$\sum x$ = **26018.53**	$\sum y$ = **27862.85**	$\sum x^2$ = **471001043.4**	$\sum y^2$ = **278086557.1**
Mean = **4336.42**	Mean = **4643.81**		

$m_x - m_y$ = 4643.81 – 4336.42 **= 307.39**

sd_x = $\sqrt{}$ [(471001043.1 – 112827317)/5] **= 8463.73**

sd_y = $\sqrt{}$ [(278086557.1 – 129389735)/5] **= 5453.38**

:. $SED_{mx - my}$ = $\sqrt{}$ [$(8463.73)^2/6 + (5453.38)^2/6$] **= 4110.4**

:. t = 307.39/4110.4

:. t = 0.07

:. Control 14.5 and Control 16.5 are not significantly different

b.) Citral 14.5 and Citral 16.5

Citral 14.5 (x)	**Citral 16.5 (y)**	**$(x)^2$**	**$(y)^2$**
33970.62	880.40	1154003023	775104.16
45292.98	23170.50	2051454037	536872070.3
576.43	10535.71	332271.54	111001185.2
14.75	4.94	217.56	24.40
33947.10	697.47	1152405598	486464.40
47544.80	2626.63	2260508007	6899185.16
$\sum x$ = **161346.63**	$\sum y$ = **38404.71**	$\sum x^2$= **6618703154**	$\sum y^2$ = **656034033.6**
Mean = **26891.10**	Mean = **6400.76**		

$m_x - m_y$ = 26891.10 – 6400.76 = **20490.34**

sd_x = $\sqrt{}$ [(6618703154 – 4338789169)/5] = **21353.75**

sd_y = $\sqrt{}$ [(656034033.6 – 245820291.7)/5] = **9057.91**

:. $SED_{mx - my}$ = $\sqrt{}$ $[(21353.75)^2/6 + (9057.911)^2/6]$ = **9469.47**

:. t = 20490.34/9469.47

:. t = 2.20

:. There is a marginally significant difference between Citral 14.5 and Citral 16 1/2

c.) Wortmannin 14.5 and Wortmannin 16.5

Wortmannin 14.5 (x)	**Wortmannin 16.5 (y)**	**$(x)^2$**	**$(y)^2$**
9809.75	199.33	96231195.06	39732.45
147.34	177.05	21709.08	31346.70
16169.64	946.86	261457257.7	896543.86
917.14	82.48	841145.80	6802.95
5.30	56.45	28.09	3186.60
20.99	519.87	440.58	270264.82
$\sum x$ = **27070.16**	$\sum y$ = **1925.56**	$\sum x^2$ = **358551776.3**	$\sum y^2$ = **1247877.38**
Mean = **4511.70**	Mean = **320.93**		

$m_x - m_y$ = 4511.70 – 320.93 = **4190.77**

sd_x = $\sqrt{}$ [(358551776.3 – 122132260.4)/5] = **6876.33**

sd_y = $\sqrt{}$ [(1247877.38 – 617963.55)/5] = **354.94**

:. $SED_{mx - my}$ = $\sqrt{}$ [$(6876.33)^2/6 + (354.94)^2/6$] = **2810.99**

:. t = 4190.77/2810.99

:. t = 1.49

:. No statistical significant difference between Wortmannin 14.5 and Wortmannin 16.5

d.) Control 14.5 and Citral 14.5

Control 14.5 (x)	**Citral 14.5 (y)**	**$(x)^2$**	**(y^2)**
921.60	33970.62	849346.56	1154003023
59.76	45292.98	3571.26	2051454037
21424.89	576.43	459025911.5	332271.54
62.90	14.75	3956.41	217.56
222.40	33947.10	49461.76	1152405598
3326.98	47544.80	11068795.92	2260508007
$\sum x$ = **26018.53**	$\sum y$ = **161346.63**	$\sum x^2$ = **471001043.4**	$\sum y^2$= **6618703154**
Mean = **4336.42**	Mean = **26891.10**		1154003023

$m_x - m_y$ = 4336.42 – 26891.10 **= 22554.68**

sd_x = $\sqrt{}$ [(471001043.4 – 112827317.2)/5] = **8463.73**

sd_y = $\sqrt{}$ [(6618703154 - 4338789169)/5] = **21353.75**

:. $SED_{mx - my}$ = $\sqrt{}$ [$(8463.73)^2$/6 + $(21353.75)^2$/6] = **9377.43**

:. t = 22554.68/9377.43

:. t = 2.41

:. There is a marginally significant difference in amelogenin expression between the 14.5 day Control and 14.5 day Citral treated molras

e.) Control 14.5 and Wortmannin 14.5

Control 14.5 (x)	**Wortmannin 14.5 (y)**	**$(x)^2$**	**$(y)^2$**
921.60	9809.75	849346.56	96231195.06
59.76	147.34	3571.26	21709.08
21424.89	16169.64	459025911.5	261457257.7
62.90	917.14	3956.41	841145.80
222.40	5.30	49461.76	28.09
3326.98	20.99	11068795.92	440.58
$\sum x$ = **26018.53**	$\sum y$ = **27070.16**	$\sum x^2$ = **471001043.4**	$\sum y^2$ = **358551776.3**
Mean = **4336.42**	Mean = **4511.70**		

$m_x - m_y$ = 175.28

sd_x = $\sqrt{}$ [(471001043.4 – 112827317.2)/5] = **8463.73**

sd_y = $\sqrt{}$ [(358551716.3 – 122132260.4)/5] = **6876.33**

:. $SED_{mx - my}$ = $\sqrt{}$ [$(8463.73)^2/6 + (6876.33)^2/6$] = **4452.0**

:. t = 175.28/4452.0

:. t = 0.04

:. There is a no significant difference in amelogenin m-RNA synthesis between Control 14.5 and Wortmannin 14.5

f.) Control 16½ and Citral 16.5

Control 16.5 (x)	**Citral 16.5 (y)**	**$(x)^2$**	**$(y)^2$**
114.80	880.40	13179.04	775104.16
8761.73	23170.50	76767912.59	536872070.3
29.91	10535.71	894.61	111001185.2
56.77	4.94	3222.83	24.40
6080.61	697.47	3697381.97	486464.40
12819.03	2626.63	164327530.1	6899185.16
$\sum x$ = **27862.85**	$\sum y$ = **38404.71**	$\sum x^2$ = **278086557.1**	$\sum y^2$ **= 656034033.6**
Mean = **4643.81**	Mean = **6400.76**		

$m_x - m_y$ = 4643.81 – 6400.76 **= 1756.95**

sd_x = $\sqrt{}$ [(278086557.1 - 129389735)/5] = **5453.38**

sd_y = $\sqrt{}$ [(656034033.6 – 245820291.7)/5] = **9057.75**

:. $SED_{mx - my}$ = $\sqrt{}$ [$(5453.38)^2$/6 + $(9057.75)^2$/6] = **4316.29**

:. t = 1756.95/4316.29

:. t = 0.41

:. No statistical significant difference in amelogenin expression between Control 16½ and Citral 16.5

g.) Control 16.5 and Wortmannin 16.5

Control 16.5 (x)	**Wortmannin 16.5 (y)**	**$(x)^2$**	**$(y)^2$**
114.80	199.33	13179.04	39732.45
8761.73	177.05	76767912.59	31346.70
29.91	946.86	894.61	896543.86
56.77	82.48	3222.83	6802.95
6080.61	56.45	3697381.97	3186.60
12819.03	519.87	164327530.1	270264.82
$\sum x$ = **27862.85**	$\sum y$ = **1925.56**	$\sum y^2$ = **278086557.1**	$\sum y^2$ = **1247877.38**
Mean = **4643.81**	Mean = **320.93**		

$m_x - m_y$ = 4643.81 – 320.93 **= 4322.88**

sd_x = $\sqrt{}$ [(278086557.1 - 129389735)/5] = **5453.38**

sd_y = $\sqrt{}$ [(1247877.38 – 617963.55)/5] = **354.94**

:. $SED_{mx - my}$ = $\sqrt{}$ [$(5453.38)^2$/6 + $(354.94)^2$/6] = **2231.04**

:. t = 4322.88/2231.04

:. t = 1.93

:. No statistical significant difference between Control 16.5 and Wortmannin 16.5

2. t-test analysis (laminin α5 expression)

a.) Control 14.5 and Control 16.5

Control 14.5 (x)	**Control 16.5 (y)**	**$(x)^2$**	**$(y)^2$**
188.97	0.89	35709.66	0.7921
772941.66	87864.94	$5.9x10^{11}$	7720247681
117.30	3499.66	13759.30	12247620.12
1666.96	43.23	2778755.64	1868.83
138.43	3970.21	19162.86	15762567.44
7281.40	464719.29	53018785.96	$2.1x10^{11}$
$\sum x$ = **780834.72**	$\sum y$ = **560098.22**	$\sum x^2$ = **$5.9x10^{11}$**	$\sum y^2$ = **$2.1x10^{11}$**
Mean = **130139.12**	Mean = **93349.70**		

$m_x - m_y$ = 130139.12 – 93349.70 = **36789.42**

sd_x = $\sqrt{}$ [$(5.9x10^{11} - 1.0x10^{11})/5$] = **312532.51**

sd_y = $\sqrt{}$ [$(2.1x10^{11} - 5.2x10^{10})/5$] = **17760.49**

:. $SED_{mx - my}$ = $\sqrt{}$ [$(312532.51)^2/6 + (17760.49)^2/6$] = **146753.51**

:. t = 36789.42/146753.51

:. t = 0.25

:. There is no significant difference between Control 14.5 and Control 16.5

b.) Citral 14.5 and Citral 16.5

Citral 14.5 (x)	**Citral 16.5 (y)**	**$(x)^2$**	**$(y)^2$**
23854.93	9809.75	569057685.3	96231195.06
10.26	620469.20	105.27	$3.8x10^{11}$
193.47	376.90	37430.64	142053.61
3.71	92361.25	13.76	8530600502
29634.70	424.02	878215444.1	179792.96
6347.62	65536.0	40292279.66	429496.73
$\sum x$ = **60044.69**	$\sum y$ = **788977.12**	$\sum x^2$ = **1487602959**	$\sum y^2$ = **$3.8x10^{11}$**
Mean = **10007.45**	Mean = **131496.19**		

$m_{x-}m_y$ = 131496.19 – 10007.45 = **121488.74**

sd_x = $\sqrt{}$ [(1487602959 – 600894132.9)/5] = **13316.97**

sd_y = $\sqrt{}$ [($3.8x10^{11}$ – $1.0x10^{11}$)/5] = **235054.27**

:. SED_{mx-my} = $\sqrt{}$ [$(13316.97)^2/6$ + $(235054.27)^2/6$] = **96114.38**

:. t = 121488.74/96114.38

:. t = 1.26

:. There is no significant difference between Citral 14.5 and Citral 16.5

c.) Wortmannin 14.5 and Wortmannin 16.5

Wortmannin 14.5 (x)	**Wortmannin 16.5 (y)**	**$(x)^2$**	**$(y)^2$**
43.77	277860.26	1915.81	$7.7x10^{10}$
205674.01	46405.24	$4.2x10^{10}$	2153446299
721.10	232.50	519841	54056.30
656301.86	12.27	$4.3x10^{11}$	150.55
1.61	28036.14	2.59	786025146.1
221.78	142.62	49186.37	20340.46
$\sum x$ = **862964.13**	$\sum y$ = **352689.03**	$\sum x^2$ = **$4.2x10^{11}$**	$\sum y^2$ = **$7.9x10^{10}$**
Mean = **143827.36**	Mean = **58781.51**		

$m_x - m_y$ = 143827.36 – 58781.51 **= 85045.85**

sd_x = $\sqrt{}$ $[(4.2x10^{11} – 1.2x10^{11})/5]$ = **243262.1**

sd_y = $\sqrt{}$$[(7.9x10^{10} – 2.0x10^{10})/5]$ = **107952.21**

:. $SED_{mx - my}$ = $\sqrt{}$$[(24326.1)^2/6 + (107952.21)^2/6]$ = **108650.91**

:. t = 85045.85/108650.91

:. t = 0.78

:. There is no significant difference between Wortmannin 14.5 and Wortmannin 16.5

d.) Control 14.5 and Citral 14½

Control 14.5 (x)	**Citral 14.5 (y)**	**$(x)^2$**	**$(x)^2$**
188.97	23854.93	35709.66	569057685.3
772941.66	10.26	$5.9x10^{11}$	105.27
117.30	193.47	13759.30	37430.64
1666.96	3.71	2778755.64	13.76
138.43	29634.70	19162.86	878215444.1
7281.40	6347.62	53018785.96	40292279.66
$\sum x$ = **780834.72**	$\sum y$ = **60044.69**	$\sum x^2$ = **$5.9x10^{11}$**	$\sum x^2$ = **1487602959**
Mean = **130139.12**	Mean = **10007.45**		

$m_x - m_y$ = 130139.12 – 10007.45 **= 120131.67**

sd_x = $\sqrt{}$ [$(5.9x10^{11} - 1.0x10^{11})/5$] = **312532.51**

sd_y = $\sqrt{}$ [(1487602959 – 600894132.9)/5] = **13316.97**

:. $SED_{mx - my}$ = $\sqrt{}$ [$(312532.51)^2/6 + (13316.97)^2/6$] = **127706.70**

:. t = 0.94

:. There is no significant difference in laminin expression between Control 14.5 and Citral 14½

e.) Control 16.5 and Citral 16.5

Control 16.5 (x)	**Citral 16.5 (y)**	**$(x)^2$**	**$(y)^2$**
0.89	9809.75	0.7921	96231195.06
87864.94	620469.20	7720247681	$3.8x10^{11}$
3499.66	376.90	12247620.12	142053.61
43.23	92361.25	1868.83	8530600502
3970.21	424.02	15762567.44	179792.96
464719.29	65536.0	$2.1x10^{11}$	429496.73
$\sum x$ = **560098.22**	$\sum y$ = **788977.12**	$\sum x^2$ = **$2.1x10^{11}$**	$\sum y^2$ = **$3.8x10^{11}$**
Mean = **93349.70**	Mean = **131496.19**		

$m_x - m_y$ = 93349.70 – 131496.19 **= 38146.50**

sd_x = $\sqrt{}$ [$(2.1x10^{11} – 5.2x10^{10})/5$] = **17760.49**

sd_y = $\sqrt{}$ [$(3.8x10^{11} – 1.0x10^{11})/5$] = **235054.27**

:. $SED_{mx - my}$ = $\sqrt{}$ [$(17760.49)^2/6 + (235054.27)^2/6$] = **96234.04**

:. t = 0.40

:. There is no significant difference in laminin expression between Control 16.5 and Citral 16.5

f.) Control 14.5 and Wortmannin 14.5

Control 14.5 (x)	**Wortmannin 14.5 (y)**	**$(x)^2$**	**$(y)^2$**
188.97	43.77	35709.66	1915.81
772941.66	205674.01	$5.9x10^{11}$	$4.2x10^{10}$
117.30	721.10	13759.30	519841
1666.96	656301.86	2778755.64	$4.3x10^{11}$
138.43	1.61	19162.86	2.59
7281.40	221.78	53018785.96	49186.37
$\sum x$ = **780834.72**	$\sum y$ = **862964.13**	$\sum x^2$ = **$5.9x10^{11}$**	$\sum y^2$ = **$4.2x10^{11}$**
Mean = **130139.12**	Mean = **143827.36**		

$m_x - m_y$ = 130139.12 – 143827.36 **= 13688.24**

sd_x = $\sqrt{}$ [$(5.9x10^{11} – 1.0x10^{11})/5$] = **312532.51**

sd_y = $\sqrt{}$[$(4.2x10^{11} – 1.2x10^{11})/5$] = **243262.1**

:. $SED_{mx - my}$ = $\sqrt{}$[$(312532.51)^2/6 + (243262.1)^2/6$] = **16185.40**

:. t = 0.86

:. There is no significant difference in laminin expression between Control 14.5 and Wortmannin 14.5

g.) Control 16.5 and Wortmannin 16.5

Control 16.5 (x)	**Wortmannin 16.5 (y)**	**$(x)^2$**	**$(y)^2$**
0.89	277860.26	0.7921	$7.7x10^{10}$
87864.94	46405.24	7720247681	2153446299
3499.66	232.50	12247620.12	54056.30
43.23	12.27	1868.83	150.55
3970.21	28036.14	15762567.44	786025146.1
464719.29	142.62	$2.1x10^{11}$	20340.46
$\sum x$ = **560098.22**	$\sum y$ = **352689.03**	$\sum x^2$ = **$2.1x10^{11}$**	$\sum y^2$ = **$7.9x10^{10}$**
Mean = **93349.70**	Mean = **58781.51**		

$m_x - m_y$ = 93349.70 – 58781.51 **= 34568.19**

sd_x = $\sqrt{}$ [$(2.1x10^{11} – 5.2x10^{10})/5$] = **17760.49**

sd_y = $\sqrt{}$[$(7.9x10^{10} – 2.0x10^{10})/5$] = **107952.21**

:. $SED_{mx - my}$ = $\sqrt{}$[$(17760.49)^2/6 + (107952.21)^2/6$] = **44663.78**

:. t = 0.77

:. There is no significant difference in laminin expression between Control 16.5 and Wortmannin 16.5